Giant moment and ferromagnetism in dilute Pd(Mn) alloys

W. M. Star*†

Francis Bitter National Magnet Laboratory,‡ Massachusetts Institute of Technology, Cambridge, Massachusetts 02139 and Kamerlingh Onnes Laboratorium, University of Leiden, Leiden, The Netherlands§

S. Foner and E. J. McNiff, Jr.

Francis Bitter National Magnet Laboratory,‡ Massachusetts Institute of Technology, Cambridge, Massachusetts 02139

(Received 23 December 1974)

The magnetization σ of a series of Pd(Mn) alloys has been measured as a function of concentration c (0.05-at.% Mn $\leq c \leq$ 2.45-at.% Mn), temperature ($1.4 \leq T \leq 260$ K) and applied field ($0 \leq H \leq 210$ kOe). The average saturation moment (for $c \leq 0.49$-at.% Mn) is $\mu_{sat} = 7.5\mu_B$/Mn. The saturation moment is consistent with the effective moment obtained from the low-field susceptibility (which obeys the Curie-Weiss law) provided that we take $S = 5/2$ (from the specific heat) and $g_{eff} = \mu/S \approx 3$. For $c \lesssim 0.23$-at.% Mn and $T \gtrsim 3.5\Theta$ the magnetization as a function of T and H is well described by the molecular-field model (with $S = 5/2$ and $g_{eff} \approx 3$) without any adjustable parameters. The magnetic field dependence of the specific heat yields an independent measure of the magnetic moment of Mn, which agrees with the magnetization data, and thus also leads to an enhanced effective g value. For the most concentrated alloys 210 kOe is not quite sufficient to saturate the solute magnetization. This is attributed to near-neighbor (Mn-Mn) antiferromagnetic interactions. Curie temperatures (T_C) and Curie-Weiss temperatures (Θ) were measured and compared with data from the literature and with corresponding data on Pd(Fe) and Pd(Co). Up to 1 at.% the variations of T_C vs c are similar for Pd(Mn), Pd(Fe), and Pd(Co), and the variations of Θ vs c are also similar. A plot of σ^2 vs H_i/σ (H_i is the internal field) for Pd(1.3-at.% Mn) shows that the magnetic transition is very sharp with a width comparable to that of the specific-heat cusp (i.e., less than 1% of T). The spontaneous magnetization of three Pd(Mn) alloys was measured as a function of T and the coefficient of the low-temperature $(T/T_C)^{3/2}$ term yielded a value for the spin-wave stiffness constant $D \approx 0.7\, T_C$ Å^{2}K, in agreement with the results obtained by others from the magnetoresistance. The spontaneous magnetization and the high-field saturation behavior are used to estimate the energy of direct antiferromagnetic interactions between the neighboring Mn atoms ($E_{int}/k_B \approx 55$ K) and the number n of sites involved ($n \approx 35$). The magnetic susceptibility of Pd(1-at.% Re) $= 4.30 \times 10^{-6}$ emu/g at 4.2 K was determined for comparison with isoelectronic Pd(Mn) alloys.

I. INTRODUCTION

In dilute Pd(Fe) and Pd(Co) alloys very large magnetic moments have been observed: about $10\mu_B$ per solute atom.[1,2] These "giant moments" are a result of the long-range positive d-electron polarization around local magnetic moments dissolved in metals with a strongly exchange-enhanced Pauli susceptibility (χ_P).[3] This polarization also causes ferromagnetism to occur in giant-moment alloys at very low impurity concentrations: for 0.2-at.% solute concentration Pd(Fe) or Pd(Co) alloys are still ferromagnetic at liquid-helium temperature. Giant moments have also been observed in Pt-base[4] and Ni_3Ga-base[5] dilute alloys, and the magnitudes of the moments scale qualitatively with χ_P.

Until very recently,[6] the observation of giant moments had been reported only for the solutes Fe and Co. Of the other first-row transition elements, only Mn has a local moment in Pd. Ti and V are nonmagnetic, and Cr and Ni are weakly magnetic with a relatively high Kondo or spin-fluctuation temperature, respectively.[7,8] Since dilute Pd(Mn) alloys were known to be ferromagnetic,[11] some host polarization was to be expected. Indeed, from the susceptibility of a Pd(3-at.% Mn) alloy Shaltiel *et al.*[11] inferred an enhancement of the solute moment. However, the only other low-temperature susceptibility result available[13] yielded a Mn moment that was only 10% higher than the free-ion value for Mn. Furthermore, for equal solute concentration (≈ 1 at.%) the Curie temperature of a dilute Pd(Mn) alloy is about a factor of 10 lower than for Pd(Fe).[12] This, together with theoretical estimates[9,10] suggested that Mn had no giant moment in Pd.

Recently, extensive investigations have been reported on the electrical resistivity,[14] magnetoresistivity,[15] and specific heat[16] of dilute Pd(Mn) alloys. The interpretation of the results suffered from the lack of magnetization data. The present paper fills this gap. Our interest in the Pd(Mn) system developed from the specific-heat measurements of Boerstoel *et al.*[16] These authors found an unusually sharp (for a dilute alloy) cusp anomaly at the Curie temperature. Furthermore, they found that the specific-heat data in external magnetic fields for alloys up to 0.5-at.% Mn could be fitted rather well with the molecular-field model

(MFM), in contrast to Pd(Fe) and Pd(Co) alloys.

In this paper we report on an extensive investigation of the magnetization σ of dilute Pd(Mn) alloys as a function of concentration ($0.05 \leq c \leq 2.5$ at.%), temperature ($1.4 \leq T \leq 260$ K) and applied field ($0 \leq H \leq 210$ kOe). Preliminary data have been reported in two previous publications.[6,17] Our most important result is that Mn has a giant moment $\mu \approx 7.5\mu_B$ in Pd and that magnetization and specific-heat data are consistent only for a spin $S = \frac{5}{2}$ and an effective g value $g_{\text{eff}} = \mu/S \approx 3$. For Mn in Pd, at least, this resolves the long-standing question of whether g, S, or both g and S of a giant moment are enhanced. In Sec. II the sample preparation and apparatus are discussed. In Sec. III the saturation behavior of the magnetization is reported. In Sec. IV the effective moment is evaluated from the low-field susceptibility measurements and is shown to be consistent with the saturation moment. In Sec. V the magnetization as a function of temperature and field is compared with the molecular-field model (using $S = \frac{5}{2}$ and $g_{\text{eff}} = \mu/S$). In Sec. VI the magnetization is compared with specific-heat data. In Sec. VII Curie temperatures (T_C) and Curie-Weiss temperatures (Θ) are compared with data from the literature. The spontaneous magnetization and the high-field magnetization of some alloys are discussed and interpreted assuming the existence of antiferromagnetically as well as ferromagnetically interacting Mn atoms. Brief remarks on related EPR data are given in Sec. VIII.

II. EXPERIMENTAL DETAILS

A. Samples

The Pd(Mn) alloys used in our investigation are listed in Table I. The three most concentrated alloys were prepared by melting together appropriate amounts of the pure constituents. The other alloys were made from a master alloy. Melting was performed in Al_2O_3 crucibles in an induction furnace under 2 atm of purified argon. The concentrations listed in Table I were obtained by chemical analysis, with the exception of the 0.05-at.%-Mn alloy for which atomic absorption was employed. In all cases the analyzed concentrations differed by no more than 10% from the nominal values. Cylindrical samples, each weighing about 1 g, were spark cut from the ingots. As indicated, two of the alloys were used previously for specific-heat measurements. These alloys have been homogenized for a long time in order to narrow the ferromagnetic transition. We refer the reader to Boerstoel *et al.*[16] for more details.

TABLE I. Sample-preparation data.[a]

at.% Mn (analysis)	Melting time	Annealing hours	Annealing °C	Cooling after annealing
2.45	5+10	48, 220	1025, 1000	q[b]
1.35	5+10	65, 220	1050, 1025	q[b]
0.96	10+3	3	500	sl
0.49	10+3	3	500	sl
0.23	10	3	500	sl
0.08	10	3	500	sl
0.054	10	3	500	sl
0.05	10+10	$\frac{1}{2}$	just below melting point	sl

[a] Starting materials (all obtained from Johnson and Matthey): Pd-S8750, Pd-S56291GF, Mn-S6759. Analysis of Pd-S8750 used for 2.45- to 0.054-at.%-Mn alloys: 8-ppm Si, other elements less than 1 ppm. Analysis of Pd-S56291GF used for 0.05-at.%-Mn alloy: 5-ppm Si, 3-ppm Fe, other less than 1 ppm. q, quenched in water; sl, slowly cooled to room temperature. 5+10: melted during 5 min., inverted, and remelted during 10 min.

[b] See also Boerstoel's paper (Ref. 16) on the specific heat.

B. Magnetization and temperature measurements

Magnetization was measured in applied fields up to 54 kG with a commercial vibrating-sample magnetometer[18] (VSM) adapted to a superconducting solenoid, so that the sample vibration was parallel to the field. For measurements in the liquid-helium temperature range the sample was mounted on a Pyrex vibration rod inside a sealed brass tube filled with ^{4}He gas.

Measurements at temperatures above 4.2 K were performed in an apparatus similar to the ^{3}He Dewar described by Oliveira and Foner.[19] For our purpose the ^{4}He insert Dewar was removed and the "^{3}He Dewar" was filled with ^{4}He gas and immersed directly into the ^{4}He, which cooled the magnet. The sample is thus cooled by conduction from the thermal link (4) (which in our case was stainless steel) downward (see Fig. 1 of Ref. 19). The equilibrium temperature at the sample during the vibration is about 4.5 K, when the bath is at 4.2 K. Temperatures closer to or a little below 4.2 K were attained by pumping on the helium in the magnet Dewar. In order to reach temperatures above 4.5 K the spacer 11 (Fig. 1 of Ref. 19) was made in the shape of a coil form, closely but smoothly fitting inside the inner tube of the apparatus. A thin brass wire wound noninductively on the coil form (resistance 120 Ω) served as a heater. With the magnet Dewar filled with liquid He, room temperature could be reached with only 0.2 W heater power.

Temperatures up to 80 K were measured with a ground-off Ohmite carbon resistor, glued to the

vibration rod between the heater and the sample. The resistor was calibrated using a CryoCal germanium thermometer. The calibration of the carbon resistor did not change during vibration, even if the experiment lasted several days. Temperature homogeneity in the space below the heater was checked with two germanium thermometers up to 20 K. Over a distance of ± 1.5 cm about the sample position, temperature differences were within the calibration errors stated by the manufacturers of the thermometer, i.e., less than 0.1% of T. The gradients were probably even smaller. The temperature was controlled with a glass-ceramic capacitance sensor[20,21] (also mounted on the vibration rod between sample and heater) with matching electronics.[22]

Temperatures above 80 K were measured with a chromel-constantan thermocouple mounted on the vibration rod. In this case magnetization data were corrected for the (small) contribution of the thermocouple moment. In all other cases the contributions of heater, thermometer, and temperature control sensor to the VSM signal were negligible.

Magnetizations in fields above 54 kOe (up to 210 kOe) were measured with the very-low-frequency vibrating-sample magnetometer[23] (VLFVSM) in water-cooled Bitter solenoids. In this case the sample was immersed in liquid helium and data were usually taken at 4.2 and 1.4 K.

The relative precision of the VSM data is better than 0.5% and that of the VLFVSM data about 1%. The absolute accuracy is determined by the calibration of the system against an Fe or Ni standard sample,[24] which may add 1% to the over-all error (but not to the relative error). Temperature errors were negligible.

III. HIGH-FIELD MAGNETIZATION

A. Experimental results

The magnetization of the two most dilute Pd(Mn) alloys was only measured up to 54 kOe and at several temperatures down to 1.4 K. The magnetizations of the other samples were also measured with the VLFVSM. Measurements up to 150 kOe were performed at 1.4 K and measurements up to 210 kOe at 4.2 K.[25] The VLFVSM data were scaled to the VSM data at lower fields, because the VSM permits a more accurate calibration.

As a function of Mn concentration the saturation behavior of the magnetization is as follows. The solute magnetization of the three most dilute alloys saturates "normally," i.e., as expected on the basis of the Brillouin function. For Pd(0.23-at% Mn) at 1.4 K saturation is almost achieved in 54 kOe, but about 70 kOe was necessary for full saturation. The solute magnetization was considered to be saturated when (i) σ was a linear function of H over a field range of about 50 kOe (somewhat less or more depending on the precision of the data), and (ii) $d\sigma/dH$ at maximum field was equal to or a little smaller than the susceptibility of pure Pd [$\chi_{Pd} = (6.85 \pm 0.1) \times 10^{-6}$ emu/g below 10 K].[26] As can be seen in Fig. 1 and Table II this criterion could still be satisfied for Pd(0.49-at.% Mn), although more than 150 kOe was needed. We define χ_{HF} as the slope $d\sigma/dH$ in the region of saturated solute magnetization, which should be equal to the matrix susceptibility χ_0 of the alloy. When nonmagnetic impurities (with the exception of Rh, and Ni if the latter is to be called nonmagnetic) are added to Pd, the susceptibility decreases.[27,28] The same is true for χ_{HF} of dilute *magnetic* Pd alloys.[28] One might therefore expect χ_{HF} of Pd(0.49-at.% Mn) to be smaller than χ_{Pd} (e.g., $\chi_{HF} \approx 6.5 \times 10^{-6}$ emu/g) whereas χ_{HF} is close to that of Pd. The plot in Fig. 1 shows that saturation is achieved so that the value of χ_{HF} is apparently not much changed by Mn at this concentration. An independent measure of χ_{HF} will be obtained from the low-field susceptibility in Sec. IV.

The Pd(0.96-at.% Mn) data in Fig. 2 and Table II suggest that in this alloy the solute magnetization is nearly saturated at 210 kOe and that above 0.96-at.% Mn this field is not sufficient to achieve saturation. It appears that Pd(1.35-at.% Mn) may still be close to saturation, but that Pd(2.45-at.% Mn) is clearly not saturated at 210 kOe.

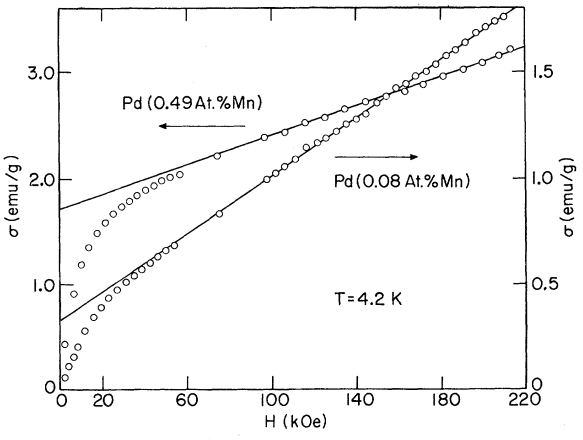

FIG. 1. Field dependence of the magnetization of Pd(0.08-at.% Mn) and Pd(0.49-at.% Mn) at $T = 4.2$ K. The straight lines represent the high-field susceptibility χ_{HF}.

TABLE II. High-field magnetization data of Pd(Mn). [a]

Alloy (at.% Mn)	T (K)	H_{max} (kOe)	χ_{HF} (10^{-6} emu/g)	σ_0 (emu/g)	μ_{sat} (μ_B/Mn)
0.05	1.38	54	6.9	0.181	6.9
0.054	1.36	54	6.9	0.222	7.8
0.08	4.2	210	6.8	0.33	7.8_6
0.23	4.2	210	6.8	0.90	7.4_5
0.49	4.2	210	6.8	1.72	6.7
0.96	4.2	210	$\lesssim 6.5$	3.48	$\gtrsim 6.9$
1.35	4.2	210	< 6.3	4.75	> 6.7
2.45	4.2	210	< 8.5	7.4	> 5.7

[a] χ_{HF} is the slope $d\sigma/dH$ in the region of saturated solute magnetization. When saturation was not achieved (as indicated in the columns for χ_{HF} and μ_{sat}) $d\sigma/dH$ at maximum applied field is reported. σ_0 is obtained from the intersections of these high-field tangents with the σ axis (Figs. 1 and 2). μ_{sat} is the saturation moment per solute atom. The values reported were obtained from σ_0.

B. Discussion of results

The specific heat[16] yields a spin $S = 2.4 \pm 0.2$ for Mn in Pd (assuming the same spin quantum number can be assigned to each Mn atom in Pd). This result suggests that the $3d$ shell of Mn in Pd is in the ^6S state, and thus a localized moment of $5\mu_B$/Mn is expected. The measured saturation moment, averaged for the first five alloys of Table II, is $7.3\mu_B$/Mn; thus Mn has a giant moment in Pd. There is some scatter in the moment data of Table II due to errors in the analysis of the Mn concentration. Using low-field susceptibility data, the concentration can be eliminated and then a more consistent set of moment data is obtained. This will be discussed in Sec. IV B.

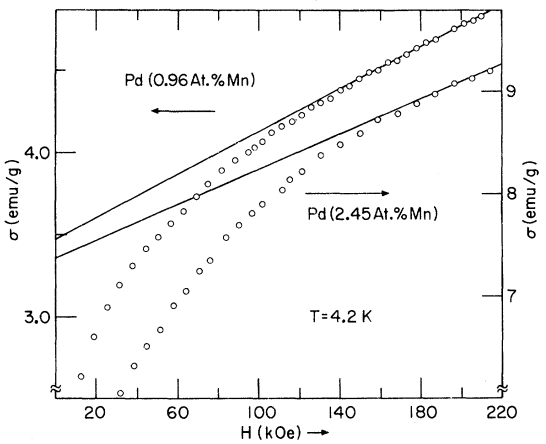

FIG. 2. Field dependence of the magnetization of Pd(0.96-at.% Mn) and Pd(2.45-at.% Mn) at $T = 4.2$ K. The straight lines represent the estimated slope $d\sigma/dH$ at the highest field.

Phenomenologically[11] as well as on the basis of theoretical models[29,30] the giant moment has been written in the form

$$\mu = g_0\mu_B S(1 + \lambda\chi_0), \quad (1)$$

where $g_0\mu_B S$ is the "bare" local moment (the symbols have their usual meaning) and the $\lambda\chi_0$ term represents the matrix polarization, which is assumed to be proportional to the matrix susceptibility χ_0 and to the local moment with proportionality constant λ. If the on-site moment of Mn in Pd is $5\mu_B$ (as the experimental spin value suggests) and $g_0 = 2$ then $\lambda_{Mn}\chi_0 \approx 0.5$. This is rather small compared to the value for Fe in Pd, where $\lambda_{Fe}\chi_0 \approx 2$.[31] From an analysis of the low-field susceptibility of Pd(3-at.% Mn) Shaltiel *et al.*[11] obtained $\lambda_{Mn}\chi_0 \approx 0.32$, which indicated the possible existence of a giant moment. However, in this analysis the value of χ_{Pd} was used for χ_0, whereas χ_0 is actually considerably lower than χ_{Pd} (see Tables II and III). Furthermore the measured effective moment[11] $p_{eff} = 6.3\mu_B$ corresponds to not more than a saturation moment, $\mu_{sat} = 5.3\mu_B$.

Considering the fact that the spin of Mn in Pd measured by specific heat is 2.4, there seems to be no matrix contribution to the spin. We will therefore represent the giant moment by means of an enhanced effective g value,

$$g_{eff} = g_0(1 + \lambda_{Mn}\chi_0) \approx 3, \quad (2)$$

for Mn in Pd. A more extensive justification for the use of this formula will be given in Sec. V (a comparison with EPR g values is given in Sec. VIII).

The progressively higher fields required to saturate the impurity magnetization when the Mn concentration increases are consistent with other properties of the Pd(Mn) system. Williams and Loram[14] obtained Curie temperatures from their resistivity data and found that dT_C/dc decreased with increasing concentration. This was attributed to the occurrence of *direct* antiferromagnetic (AF) Mn-Mn interactions (in agreement with calculations by Moriya[9]) in contrast with the *indirect* ferromagnetic interactions which are carried by the host d band. The increase of AF interactions with Mn concentration was also shown by the susceptibility measurements of Rault and Burger.[32] They found that the Curie-Weiss temperature Θ has a maximum at about 2.5-at.% Mn (see also Sec. VII A and Fig. 12), becomes zero at 8-at.% Mn, and decreases with increasing concentration, so that $\Theta = -25$ K at 25-at.% Mn, the highest concentration studied. In Sec. VII, the spontaneous and the high-field magnetizations are used to estimate the energy of direct Mn-Mn interactions and of the number of Mn atoms involved.

IV. LOW-FIELD SUSCEPTIBILITY

A. Experimental results

The initial susceptibility χ_i of all the alloys was obtained from recorder plots of the magnetization versus field. The slopes of the magnetization curves were determined in sufficiently low fields so that σ was proportional to H. The lowest measuring temperature was 1.4 K or slightly above T_C (the Curie-temperature) whichever was higher. The highest temperature was 260 K or lower, depending on whether χ_{alloy} was sufficiently large compared to χ_{Pd} to obtain a reasonably accurate value for the Mn contribution (e.g., $\Delta\chi_i/\chi_{\text{Pd}} \gtrsim 0.5$). Temperature intervals were about 10% of T. The random error in the susceptibility data is estimated to be less than 2%. Compared to this error, temperature errors are negligible. The susceptibility data were least-squares fit to the Curie-Weiss formula

$$\chi_i = \chi_0 + C/(T-\Theta), \tag{3}$$

where the Curie constant $C = Ng_{\text{eff}}^2 \mu_B^2 S(S+1)/3k_B$, N is the number of Mn atoms per gram of the alloy, and the other symbols have their usual meaning (we assume that Mn in Pd has no orbital angular momentum). The results of the Curie-Weiss fits are listed in Table III along with some derived data. Equation (3) was linearized using a trial value of Θ, writing $\Theta = \Theta_0 + \epsilon$, and expanding in terms of ϵ including only the first power of ϵ. This procedure was repeated until higher powers of ϵ could be neglected. Because the expected error in the susceptibility data is a fixed relative error, the data in the least-squares-fitting procedure have been given a weight proportional to $(\chi_i)^{-2}$, at each temperature. The least-squares program contained a procedure by which points deviating more than a fixed amount from the computed fit could be rejected. For the three most dilute alloys this tolerance was made 1%, for the others it was 2%. For the three most dilute alloys all measured points were included in the initial fit (Table III). The susceptibility of Pd is temperature dependent, showing a maximum at $T \approx 80$ K, which is about 9% above the zero-temperature susceptibility. The matrix susceptibility of the Pd(Mn) alloys may be temperature dependent as well. Therefore, an upper bound of $T = 50$ K was taken in the Curie-Weiss fit for Pd(0.23-at.% Mn) and Pd(0.49-at.% Mn).[33] The lower bound of T in these cases was determined by the same rejection procedure. For the three most concentrated alloys, the lower as well as the upper bound of T in the least-squares fit were determined by the rejection procedure. This way of choosing a range for the fit can be criticized because there is no *a priori* reason why Eq. (3) should hold. In support of our procedure we note (i) the fit is excellent in all cases over a temperature range of about a decade, and (ii) the results for the various alloys are consistent with each other and can be interpreted in a coherent fashion (Secs. IV B and V).

Figure 3 is representative for the three most dilute alloys and (in addition to Table III) shows the quality of the Curie-Weiss fits. Effects of the temperature dependence of χ_0 are illustrated in Figs. 4 and 5 and are discussed in Sec. IV B.

B. Discussion of results

The measured saturation moment $\mu_{\text{sat}} = g_{\text{eff}} S\mu_B$ and the measured effective moment $p_{\text{eff}} = g_{\text{eff}}[S(S+1)]^{1/2}\mu_B$ can be compared when the

TABLE III. Results obtained from the Curie-Weiss fits to the Pd(Mn) susceptibility data. The third column lists the total number of data points within the T range of the second column, and after the minus sign is the number of points rejected before the final fit was obtained. The fourth column gives the root-mean-square relative deviation of the data from the fit. The saturation moment μ_{sat} was obtained from the effective moment p_{eff}, assuming $S = \frac{5}{2}$. The last column lists a molecular-field constant $\gamma = \Theta/C$, according to the molecular-field model [Eq. (3)].

Alloy (at.% Mn)	Range of fit (K)	Number of points	rms deviation of fit (%)	Curie constant (10^{-6}emu/g)	Θ (K)	χ_0 (10^{-6}emu/g)	p_{eff} (μ_B/Mn)	μ_{sat} from p_{eff} (μ_B/Mn)	$\gamma = \Theta/C$ (10^3 g/emu)
0.05	1.4–4.2	11 – 0	0.2	44.6	0.180	6.91	8.71	7.36	4.04
0.054	1.4–11	20 – 2	0.4	55.4	0.241	6.91	9.34	7.89	4.35
0.08	1.4–21	29 – 3	0.6	82.3	0.387	6.81	9.35	7.91	4.70
0.23	3.6–50	45 – 0	0.7	209	1.334	6.82	8.80	7.44	6.37
0.49	6–51	29 – 0	0.6	392	2.66	6.90	8.23	6.96	6.80
0.96	8–110	37 – 0	0.6	791	4.56	6.07	8.36	7.06	5.76
1.35	8–130	44 – 1	0.7	1089	5.48	5.76	8.26	6.98	5.04
2.45	9–140	44 – 3	0.9	1716	7.12	4.36	7.67	6.48	4.15

spin is known. Based on specific-heat data (see Sec. III), we take $S=\frac{5}{2}$. Table III shows that μ_{sat} thus obtained from p_{eff} agrees well with the data in Table II. The average for the first five alloys is $7.5\mu_B$/Mn, compared to 7.3 in Table II. If the scatter in the data among the various alloys is due to errors in the concentration, this scatter can be removed by eliminating the concentration from the two equations: $\sigma_0 = NSg_{eff}\mu_B$ and $C = Ng_{eff}^2\mu_B^2 S(S+1)/3k_B$, giving $g_{eff} = 3k_BC/\sigma_0\mu_B(S+1)$. Again using $S=\frac{5}{2}$, one can also solve for the concentration. Alternatively, using the analyzed Mn concentration and eliminating g_{eff}, one can solve for S. The values c', g', and S' thus obtained are listed in Table IV. For the first five alloys σ_0 from Table II and C from Table III were used. For the last three alloys this σ_0 was probably not the true saturation magnetization (Sec. III). In order to at least partly overcome this difficulty we used the measured alloy magnetization at 210 kOe and subtracted χ_0 (from Table III) times 210 kOe, to determine σ_0'. The values of σ_0' are listed in Table IV and were used to calculate c', g_{eff}' and S'. With two exceptions c' agrees within 5% with the analyzed concentrations. These results support the procedure followed, in particular with regard to the determination of σ_0'. The moment (i.e., $g_{eff}'S$) is then a slowly decreasing function of the concentration. The average for the first five alloys is $7.7\mu_B$/Mn.

The spin values (S') presented in Table IV show considerable scatter. This is to be expected, because in this particular analysis S' is obtained from an expression of the form $(S'+1)/S' \sim \sigma_0^{-2}Cc$ (C is the Curie constant and c is the Mn concentration). An error of 5% in c is not unlikely and if $S \approx 5/2$ such an error is multiplied by 3.5 in the final result for S'. With this in mind the spin values in Table IV may be said to agree well with those obtained from the specific-heat data.[16] In

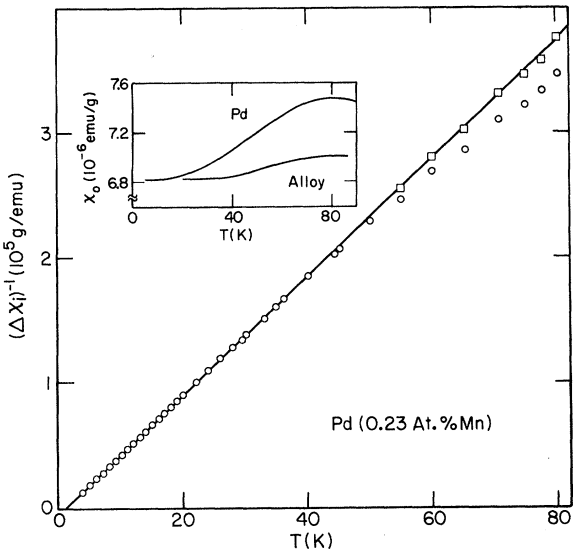

FIG. 4. Inverse of the incremental susceptibility ($\Delta\chi_i = \chi_i - \chi_0$) of Pd(0.23-at.% Mn) versus temperature. Open circles: χ_0 obtained from the Curie-Weiss fit and the straight line represents this fit. Open squares: data corrected for temperature dependent χ_0 (see text). Insert: temperature dependence of susceptibility of pure Pd and estimated matrix susceptibility of Pd(0.23-at.% Mn) used to correct $\Delta\chi_i$ above 50 K.

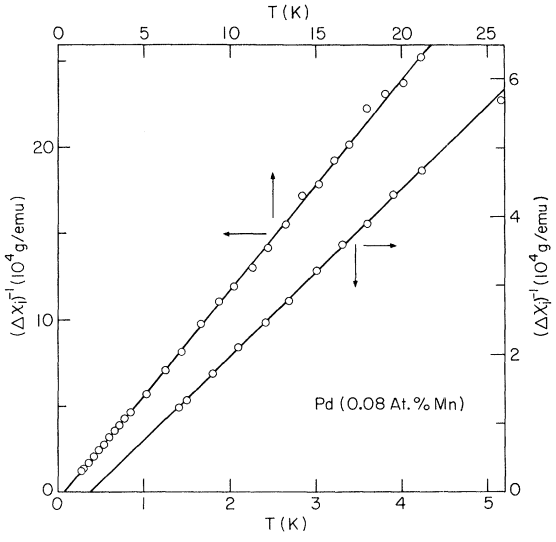

FIG. 3. Inverse of the incremental susceptibility ($\Delta\chi_i = \chi_i - \chi_0$) of Pd(0.08-at.% Mn) plotted versus temperature on two scales. χ_0 was obtained from the Curie-Weiss fit, and the straight line represents this fit.

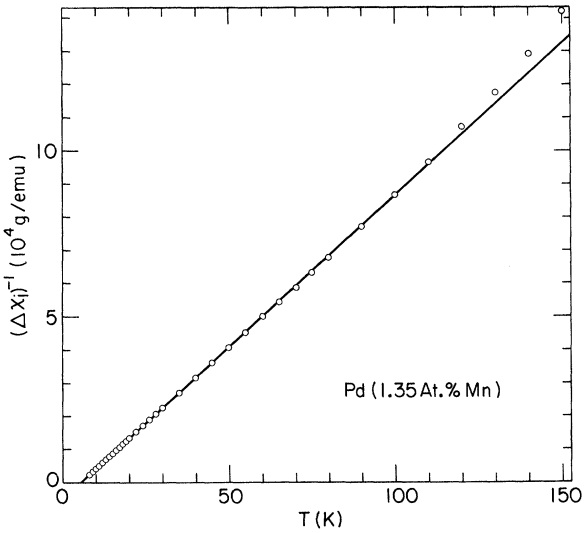

FIG. 5. Inverse of the incremental susceptibility ($\Delta\chi_i = \chi_i - \chi_0$) of Pd(1.35-at.% Mn). χ_0 obtained from the Curie-Weiss fit. The straight line represents this fit.

TABLE IV. Values of c' and g'_{eff}, the Mn concentration and effective g value calculated from the equations for the saturation moment and the Curie constant, assuming $S=\frac{5}{2}$ (see Sec. IV B). S' is the spin value obtained from the same equations using the analyzed concentrations and eliminating g_{eff}. σ'_0 is defined in Sec. IV B.

c (at.% Mn)	c' (at.% Mn)	g'_{eff}	S'	σ'_0 (emu/g)	$g'S=\mu'_{\text{sat}}$ (μ_B/Mn)
0.05	0.044	3.15	1.7	•••	7.88
0.054	0.053	3.18	2.4	•••	7.95
0.08	0.079	3.18	2.4	•••	7.95
0.23	0.23	2.97	2.5	•••	7.43
0.49	0.45	2.91	1.9	•••	7.28
0.96	0.95	2.84	2.4	3.56	7.10
1.35	1.29	2.86	2.1	4.86	7.15
2.45	2.34	2.65	2.2	8.26	6.63

particular, there is no reason to assume an enhancement of S. The enhancement of the magnetic moment of Mn in Pd can be fully accounted for by an enhancement of g. This point will be further substantiated in Secs. V and VI (for a comparison with EPR g values see Sec. VIII).

The problem of whether g or S or both g and S of a giant moment are enhanced has received considerable attention in the literature. From analyses of magnetization,[38] Mössbauer-effect,[39] and magnetoresistance[40] data large spin values were deduced, which were in disagreement with specific-heat data.[34] Takahashi and Shimizu,[29] employing a molecular-field model (MFM), analyzed magnetization data of dilute Pd(Fe) and Pd(Co) alloys. They obtained $S=\frac{3}{2}$ and $S=1$ for Fe and Co, respectively. It should be noted that in their model the enhancement of the moment can be incorporated in g. We will use the same model in Sec. V. Nieuwenhuys *et al.*[34] fitted their specific-heat data for Pd(Fe) and Pd(Co) with the MFM including a Gaussian distribution of g values. In this model also, the enhancement of the moment is accounted for by an enhancement of g only.

The method used before to obtain values for the spin of Mn in Pd from μ_{sat} combined with the Curie constant (p_{eff}) may also be applied to Pd(Fe). According to Chouteau and Tournier[2] $\mu_{\text{sat}}=g_{\text{eff}}S=10\mu_B$/Fe and $p_{\text{eff}}=g_{\text{eff}}[S(S+1)]^{1/2}=13\mu_B$/Fe, which yields $S=1.45$ (and $g_{\text{eff}}=7$), i.e., there is no enhancement of S. It would be desirable to have data on μ_{sat} and p_{eff} (measured on the same sample) for other giant-moment systems as well. A particularly interesting case is Fe in Ni_3Ga where moments as high as $84\mu_B$/Fe have been reported by Liddell and Street.[5] The hyperfine-field data obtained by these authors were analyzed assuming $g=2$, so that the giant moment was ascribed to a giant spin. For Mn in Pd we arrive at the opposite conclusion, i.e., a free-ion spin and a giant effective g value. This will be discussed further in Sec. V.

According to Table IV, $\mu_{\text{sat}}=g'_{\text{eff}}S'$ decreases with increasing Mn concentration. Such a decrease has also been observed in Pd(Fe) and Pd(Co) alloys.[41] The relative change of the d-band part of the moment as a function of Mn, Fe, or Co concentration is about the same. For the lowest concentrations of Mn in Pd (Table IV) the band part of the moment is $7.9-5=2.9\mu_B$/Mn. For the 2.45-at.%-Mn alloy the band contribution is $6.6-5=1.6\mu_B$/Mn, i.e., a decrease by 45%. For Fe in Pd the band part of the moment at very low concentration[2] is $10-3=7\mu_B$/Fe, assuming $S=\frac{3}{2}$.[31,34] For 2.5-at.% Fe in Pd the band part of the moment[36] is $8-3=5\mu_B$/Fe, a decrease by 30%.

According to Eq. (1) the band part of the moment is proportional to $\lambda\chi_0$. Regarding λ, Kim and Schwartz[37] have calculated that both the range and the amplitude of the matrix polarization should decrease when the d-band splitting increases. This would imply different values for μ_{sat} measured directly and μ_{sat} as obtained from p_{eff} (using $S=\frac{5}{2}$). However, for this effect to be important, the required bandsplitting would occur with ~1-at.% Fe in Pd or with ~3-at.% Mn in Pd, which is beyond the concentration being considered here.

The question of whether the band part of a giant moment is proportional to χ_{HF} ($=\chi_0$) was considered by Guertin and Foner.[42] These authors measured μ_{sat} of Fe in $Pd_{1-x-y}A_xB_y$ hosts (A=Ag, Pt; B=Rh) and found μ_{sat} not to be proportional to the matrix susceptibility. However, a problem with alloys in general is that the variation of the matrix susceptibility upon alloying may not be spatially uniform. In Pd(Mn) alloys Eq. (1), with χ_0 values from Table III, accounts approximately for the variation of $\mu_{\text{sat}}=g'_{\text{eff}}S$ as a function of concentration. If it is assumed that the decrease of χ_0 at the Mn sites is stronger than elsewhere, the variation of μ_{sat} with respect to the variation of χ_0 would be reduced, which seems contrary to our observations. One might hope to obtain independent information on the variation of χ_0 upon alloying in Pd(Mn) by substituting a solute that is isoelectronic with Mn and nonmagnetic in Pd, e.g., Re. For the susceptibility of Pd(1-at.% Re) we found a value of 4.30×10^{-6} emu/g, which remained constant up to $T=130$ K and then decreased slowly to 3.73×10^{-6} emu/g at $T=260$ K. This cannot be a reliable estimate for χ_0 of Pd(1-at.% Mn). When the Pd(1-at.% Re) data are used as χ_0 for Pd(0.96-at.% Mn), then the $(\Delta\chi_i)^{-1}$ vs T plot is strongly curved, with $d^2[(\Delta\chi_i)^{-1}]/dT^2<0$ (the reverse of Fig. 5, but much worse) and this is not

likely to be correct. Clearly, the idea of isoelectronic substitution does not work here. Considering that $\chi_{HF}=\chi_0$ up to 0.49-at.% Mn, χ_0 (Table III) of the remaining three alloys is probably a good approximation to the true matrix susceptibility, because (i) c and c' (obtained using χ_0: Table IV) agree quite well, and (ii) Eq. (1) holds approximately. This does not prove Eq. (1) but shows that our interpretation of the Pd(Mn) data is internally consistent.

The effect of the temperature dependence of χ_0 is illustrated in Figs. 4 and 5. The measured points above 50 K in Fig. 4 lie below the Curie-Weiss fit (for which the upper bound was fixed at 50 K) indicating that χ_0 increases with temperature. The inset in Fig. 4 shows a tentative matrix susceptibility, $\chi_0(T)$, that accounts for the data. The open squares in Fig. 4 were obtained in the following way. A trial $\chi_0(T)$ was subtracted from the experimental data. The resulting $\Delta\chi_i$ should then be proportional to $g_{\rm eff}^2=g_0^2[1+\lambda\chi_0(T)]^2$, which would lead to a deviation from the Curie-Weiss law. Therefore $\Delta\chi_i$ was multiplied by $\{[1+\lambda\chi_0(0)]/[1+\lambda\chi_0(T)]\}^2$ and the resulting $(\Delta\chi_i)^{-1}$ values were compared with the Curie-Weiss line in Fig. 4. $\chi_0(T)$ was subsequently corrected until satisfactory agreement was achieved. Although this procedure leads to unique values of $\chi_0(T)$ once $\chi_0(0)$ is known, it cannot be considered a proof of the temperature dependence of $g_{\rm eff}$ (or $p_{\rm eff}$). A neglect of this temperature dependence simply leads to different values for $\chi_0(T)$. In the present case at 80 K the temperature correction to $g_{\rm eff}^2$ is 2%. Finally, if $\chi_0(0)$ had to be smaller than 6.82×10^{-6} emu/g, $\chi_0(T)$ also would change and in particular the maximum value at 80 K would increase. The preceding analysis is intended as a qualitative guide; it shows the effect of a temperature dependence of χ_0 and indicates that the upper bound of 50 K in the Curie-Weiss fit was a reasonable choice.

If all the measured points up to 80 K are included for Pd(0.49-at.% Mn) the fit is almost equally good, but χ_0 increases by 1% to 6.97×10^{-6} emu/g and C decreases by 0.5% to 3.90×10^{-4} emu/g. This shows that a small temperature dependence of χ_0 remains here, and that the neglect of this temperature dependence up to 100 K for the remaining alloys is fully justified.

The effect of the gradual decrease of χ_0 with increasing temperature beyond 100 K is shown in Fig. 5 and has been taken care of by the rejection procedure in the Curie-Weiss-fitting program.

The same type of analysis that was used above to account for the temperature dependence of χ_0 for Pd(0.23-at.% Mn) was used by Shaltiel *et al.*[11] to account for the temperature dependence of χ_0 above 80 K in Pd(1-at.% Fe), Pd(1-at.% Co), and Pd(3-at.% Mn). Although the analysis seems qualitatively correct, these authors used $\chi_{\rm Pd}$ for χ_0. From our previous analysis we conclude that this is not a very good approximation, particularly not for Pd(3-at.% Mn) (see also Ref. 42). The values for Θ and γ listed in Table III will be discussed in Sec. VII A, along with T_C.

V. $\sigma(H,T)$-MOLECULAR-FIELD MODEL

Thus far we have only discussed the two limiting cases, $\mu H\gg k_BT$ ($\mu_{\rm sat}$) and $\mu H\ll k_BT$ ($p_{\rm eff}$). In this section we consider the intermediate region, i.e., the field dependence of the magnetization. The experimental data will be compared with the model of Takahashi and Shimizu.[29] This model can be summarized (in a slightly simplified form) as follows. The impurity moments and the d band interact with an energy

$$E=-\lambda\sigma_i\sigma_d, \tag{4}$$

i.e., a molecular field $\lambda\sigma_i$ (proportional to the local moment magnetization σ_i) acts on the itinerant d electrons (magnetization σ_d), and conversely a molecular field $\lambda\sigma_d$ acts on the local moments. When a magnetic field H is applied, the matrix magnetization (assumed to involve d electrons only) is

$$\sigma_d=\chi_0(H+\lambda\sigma_i), \tag{5}$$

where χ_0 is the matrix susceptibility. The magnetization of the (*unenhanced*) local moments is

$$\sigma_i=\sigma_{i0}B_S\left(\frac{g_0\mu_BS}{k_BT}(H+\lambda\sigma_d)\right), \tag{6}$$

where B_S is the Brillouin function for spin S, $\sigma_{i0}=Ng_0S\mu_B$ is the saturation magnetization of the (unenhanced) local moments, and the other symbols have their usual meaning. The total magnetization is

$$\sigma_{\rm tot}=\sigma_d+\sigma_i=\chi_0H+(1+\lambda\chi_0)\sigma_i. \tag{7}$$

In the argument of the Brillouin function σ_d is replaced by the right-hand side of Eq. (5) and the total magnetization then reads

$$\sigma_{\rm tot}=\chi_0H+\sigma=\chi_0H+\sigma_0B_S\left(\frac{g_{\rm eff}\mu_BS}{k_BT}(H+\gamma\sigma)\right), \tag{8}$$

where $\sigma=(1+\lambda\chi_0)\sigma_i$, $\sigma_0=Ng_{\rm eff}\mu_BS$, $g_{\rm eff}=g_0(1+\lambda\chi_0)$, and $\gamma=\lambda^2\chi_0/(1+\lambda\chi_0)^2$. According to Eq. (8) the matrix polarization caused by the local moments can be taken into account by simply replacing g_0 by an enhanced $g_{\rm eff}=g_0(1+\lambda\chi_0)$, in agreement with Eq. (1) and the discussion in Secs. III and IV. We thus find a giant moment with a "normal" spin and

a "giant" effective g value.

Equation (8) will now be compared with experimental data. All quantities needed to calculate σ with Eq. (8) are known from experiment. As before, we take $S=\frac{5}{2}$[16]; σ_0 is the saturation magnetization (Table II: σ_0), g_{eff} is obtained from the saturation magnetization and the Curie constant (Table IV: g'_{eff}), and γ is given in Table III. Figures 6 and 7 show that the agreement between the model and experiment is very good (almost within experimental error). The Brillouin function is also shown in the figures, calculated with the same parameters as the molecular-field model (MFM), but with $\gamma=0$. This gives an indication of the importance of the ferromagnetic interaction. It is clear from Figs. 6 and 7 that the MFM can only in a first approximation account for the ferromagnetic interaction. In other words, for the MFM to be adequate (e.g., a maximum difference of 3% between the data and the MFM), T must be sufficiently large compared with Θ. As a rule of thumb we can take $T\gtrsim 3.5\Theta$. For Pd(0.23-at.% Mn) below $T=4.2$ K the MFM is a poor approximation to the experimental data (Fig. 8). At $T=4.25$ K, the MFM is still not very good; at 5 K (not shown) it is better and at 9.2 K and 13.1 K the fit is quite good. In this concentration region the antiferromagnetic interaction also begins to play a role. It was mentioned in Sec. III A that even at $T=1.4$ K, $H=54$ kOe was not sufficient to fully saturate the solute magnetization of Pd(0.23-at.% Mn) and this was attributed in Sec. III B to direct AF coupling between neighboring Mn atoms. This may also

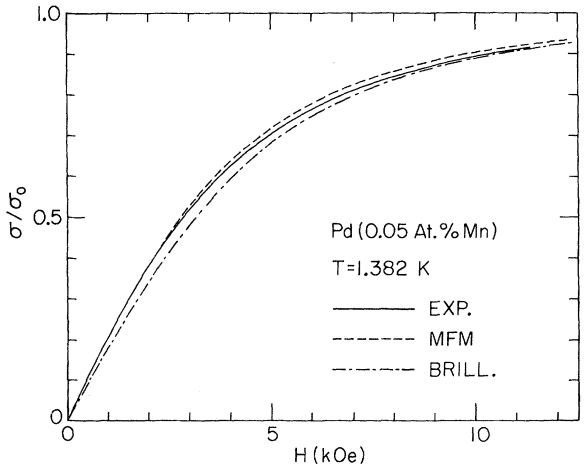

FIG. 6. Giant-moment magnetization $\sigma=\sigma_{\text{tot}}-\chi_0 H$, normalized by the saturation magnetization σ_0, of Pd(0.05-at.% Mn) versus applied field at $T=1.382$ K ($c'=0.044$-at.% Mn from Table IV is probably more reliable). The Brillouin curve was computed with the same parameters as the MFM, but with $\gamma=0$.

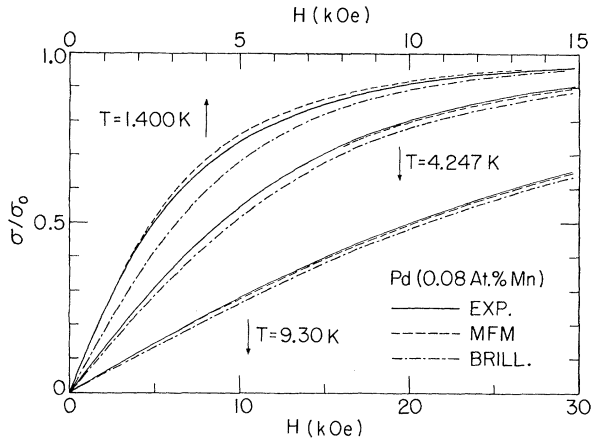

FIG. 7. Giant-moment magnetization $\sigma=\sigma_{\text{tot}}-\chi_0 H$, normalized by the saturation magnetization σ_0, of Pd(0.08-at.% Mn) versus applied field at $T=1.400$ K, $T=4.247$ K, and $T=9.30$ K. The Brillouin curves were computed with the same parameters as the MFM, but with $\gamma=0$.

explain why in Fig. 8 at 4.25 K the experimental magnetization above 40 kOe is even smaller than the free-spin magnetization, despite the ferromagnetic interaction. Anticipating the discussion in Sec. VII C we may say that in this alloy about 8% of the Mn atoms show an AF interaction with near neighbors (in addition to the longer-range ferromagnetic interaction) and that the interaction energy (in units of temperature) may be as large as 50 K. For Pd(0.49-at.% Mn) about 17% of the Mn atoms would interact antiferromagnetically, which again may explain the difference between the data and the MFM at high fields in Fig. 9 (in this case at $T=10.06$ K: $T/\Theta=3.8$). The influence

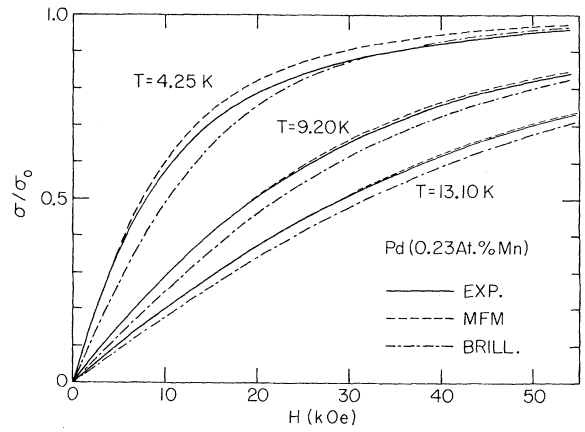

FIG. 8. Giant-moment magnetization $\sigma=\sigma_{\text{tot}}-\chi_0 H$, normalized by the saturation magnetization σ_0 of Pd(0.23-at.% Mn) versus applied field at $T=4.25$ K, $T=9.20$ K, and $T=13.10$ K. The Brillouin curves were computed with the same parameters as the MFM, but with $\gamma=0$.

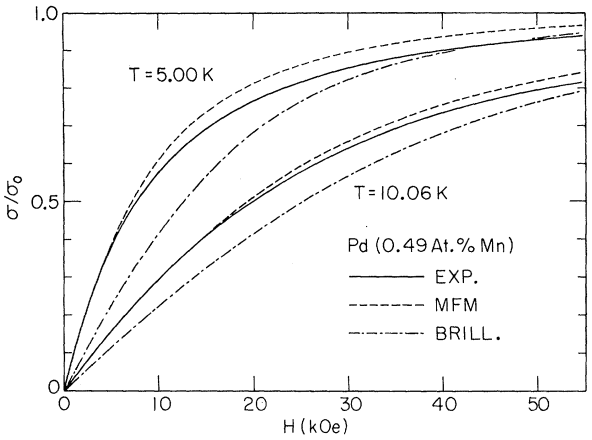

FIG. 9. Giant moment magnetization $\sigma=\sigma_{\text{tot}}-\chi_0 H$, normalized by the saturation magnetization σ_0, of Pd(0.49-at.% Mn) versus applied field at $T=5.00$ K and $T=10.06$ K ($c'=0.45$-at.% Mn from Table IV is probably more reliable). The Brillouin curves were computed with the same parameters as the MFM, but with $\gamma=0$.

of these AF interactions on the entropy (i.e., the spin) will be discussed in Sec. VII C.

If we had not fixed the spin at $S=\frac{5}{2}$, but instead had determined the spin from the best fit of the MFM to the magnetization data, as was done by other authors for Pd(Fe) (e.g., Ref. 38), a better fit could have been obtained in Figs. 6–8, but a larger spin value would result. The reason is that with a fixed saturation magnetization and a fixed Curie constant, the magnetization as a function of field (beyond the region where $\sigma \propto H$) increases more slowly for a larger spin. However, such a procedure cannot be correct for several reasons: (i) The spin obtained in this way does not agree with specific-heat data; (ii) once the spin is determined by a "best-fit" procedure, g'_{eff} and c' can be obtained from the equations for μ_{sat} and p_{eff} (Sec. IV B, Table IV). This time c' does not agree with the analyzed concentrations, however. If, e.g., $S=\frac{7}{2}$ so that $g\approx 2$ all values of c' would decrease by 10%. (iii) The "best fit" procedure to determine S attaches too much value to the model, i.e., the Brillouin function and the molecular-field approximation. There is no reason why this model should precisely fit the experimental data. Since the same arguments hold for other giant moment systems [(ii) was never checked before, except for Pd(Fe) in Sec. IV B] the large spin values reported for Fe in Pd,[38–40] and in Ni_3Ga,[5] probably reflect the inadequacy of the model used to fit the data. In general one must be very careful in extracting values for physical quantities from an analysis of experimental data using a model, such as the Brillouin function along with the MFM approximation. In particular, for the magnetization data,[38–40] the curvature of the σ vs H plots has been used to determine S, which of course is very much model dependent. In our analysis of the Pd(Mn) data all physical quantities were obtained in the low-field (p_{eff}) and high-field (μ_{sat}) limits of σ and from the entropy, which is model independent. Since our model calculations involve no adjustable parameters (i.e., no fitting), the agreement with experimental data in Figs. 6–8 supports the physical picture.

Nieuwenhuys *et al.*[34] have applied the MFM with considerable success to the specific-heat data of dilute Pd(Fe) and Pd(Co) alloys, by incorporating a Gaussian distribution of effective g values. As yet there is no independent proof of the existence of such a g-value distribution and it may be that this is just another way to hide the deficiencies of the Brillouin function and the MFM. A distribution of g values would also improve the agreement between the MFM and the Pd(Mn) data in Figs 6–8, but again this would probably overrate the model. In conclusion we can say that the MFM (involving the Brillouin function) gives a satisfactory description of the Pd(Mn) magnetization data provided $T \gtrsim 3.5\,\Theta$ and $c \lesssim 0.23$-at.% Mn.

Equation (8) leads to a relation between the Curie temperature T_c and $\lambda\chi_0$ (i.e., the giant moment) namely

$$T_C=\gamma C=\lambda^2\chi_0 C/(1+\lambda\chi_0)^2, \tag{9}$$

where $C=Ng_{\text{eff}}^2\mu_B^2 S(S+1)/3k_B$ is the Curie constant. Using $\lambda\chi_0\approx 0.5$, and $\chi_0=6.8\times10^{-6}$ emu/g we obtain $T_C=15$ K/at.% Mn, which should be compared with the experimental $\Theta\approx 5$ K/at.% Mn (Table III). The large difference is probably a result of the strong radial dependence of the matrix polarization around each solute atom.[35] In the Pd(Mn) alloys considered in the present paper, the ferromagnetically interacting Mn atoms are several nearest-neighbor distances apart so that only a fraction of the matrix polarization is effective in the interaction process. On the other hand, in the MFM the matrix polarization is uniform so that each solute atom interacts equally with all others, and the total matrix polarization is involved. Equation (9) can nevertheless be useful to compare T_C and giant-moment data of Pd(Mn) and, e.g., Pd(Fe). According to Eq. (9), $T_C \propto \lambda^2\chi_0 S(S+1)$ [the factor $(1+\lambda_0)^2$ cancels against the same factor in C]. Using $\lambda\chi_0=0.5$, $S=\frac{5}{2}$ for Pd(Mn) and $\lambda\chi_0=2$, $S=\frac{3}{2}$ for Pd(Fe) (see also Sec. IV B), Eq. (9) yields the ratio T_C (PdFe)/T_C(PdMn)≈ 16. About the same ratio is found experimentally for 1-at.% Fe or Mn in Pd. This suggests that although the magnitudes of the Pd-matrix polarizations by Mn and Fe differ considerably, the radial dependence of these polarizations is similar (at least beyond a second- or

third-nearest-neighbor distance). The latter conclusion could have been used as an assumption, to predict the giant moment of Mn in Pd long before it was measured, using Eq. (9) and the above-mentioned T_C ratio [T_C values for Pd(Mn) have been available[11] since 1964].

Dilute Pd(Gd) alloys are also ferromagnetic, with $T_C \approx 0.6$ K/at.% Gd. We determined T_C from the specific-heat maximum[43,44] in which case T_C is roughly proportional to the Gd concentration (up to 7-at.% Gd). Somewhat higher T_C values were obtained from the magnetization.[45] There are some problems with the determination of T_C in these alloys, which will be discussed in Sec. VII A. Using $S=\frac{7}{2}$[46] and Eq. (9) with T_C (PdMn)/T_C(PdGd) ≈ 10, one finds $\lambda\chi_0 \approx 0.1$ so that the total moment of Gd in Pd would be about $7.8\mu_B$. This is lower than the maximum value reported by Praddaude et al.,[47] but in good agreement with more recent analysis.

VI. COMPARISON WITH SPECIFIC-HEAT DATA

In this section we will show that the giant moment of Mn in Pd can also be obtained from the magnetic field dependence of the specific heat. Boerstoel *et al.*[16] compared their data on the specific heat of dilute Pd(Mn) alloys as a function of temperature and applied magnetic field with numerical calculations based on the molecular-field model. For $c \leq 0.5$-at.% Mn the MFM fitted data satisfactorily, provided the applied field was sufficiently large compared with the saturation molecular field. According to Boerstoel the temperature of the specific-heat maximum at fixed field, $T_{\max,H}$, computed with the MFM, is approximately a linear function of the field:

$$T_{\max,H} = \Theta[1 + H/1.50H_m(0)] \qquad (10)$$

for $S=\frac{5}{2}$. The line given by Eq. (10) fits the MFM calculation in the range $2 \leq H/H_m \leq 10$ and at $H=0$. A similar relationship is found experimentally. Thus Eq. (10) can be used to obtain $H_m(0)$, the saturation molecular field. The molecular-field constant $\gamma = H_m(0)/\sigma_0$ follows immediately. Alternatively, γ can be obtained from the Curie temperature $T_{\max,0} = \Theta$ using the MFM expression for Θ. Boerstoel noted systematic differences between the two γ values thus found for each alloy. In a footnote he suggested that significant deviations of the g value of Mn in Pd from $g=2$ might cause this inconsistency ($g=2$ was assumed throughout). This possibility was not pursued, however.

Using the MFM relationships, Eq. (10) can be written

$$T_{\max,H} = T_{\max,0} + 0.78 g_{\text{eff}} \mu_B H/k_B . \qquad (10a)$$

Comparing the slope $dT_{\max,H}/dH$ with the experimentally observed slopes yields values for g_{eff}. The average for the three most dilute alloys of Fig. 11 in Boerstoel's paper[16] is $g_{\text{eff}} = 2.9$. This is in good agreement with the magnetization and susceptibility data of Secs. III and IV.[48] Using the new effective g value removes the inconsistencies in γ mentioned above. In Table V the new molecular-field constants are listed, together with some other relevant data on Boerstoel's samples. The γ values are in reasonable agreement with those of Table III, considering the different methods by which the two sets were obtained, the simplicity of the MFM, and the fact that the concentration enters in the calculation of γ in Table V (c cancels in $\gamma = \Theta/C$, Table III). The large γ of Pd(0.08-at.% Mn) in Table V may be the result of an error in c plus the fact that for this alloy the maximum incremental specific heat is only 10% of the total. T_C and γ will be discussed further in Sec. VII A.

Turning now to Gd, a MFM calculation for $S=\frac{7}{2}$ analogously to $S=\frac{5}{2}$[16] yields

$$T_{\max,H} = T_{\max,0} + 0.98 g_{\text{eff}} \mu_B H/k_B . \qquad (11)$$

The line given by Eq. (11) fits the MFM calculation in the range $3 \leq H/H_m \leq 10$ and at $H=0$. Such a relationship has also been observed experimentally. Zwart[44] found, for Pd(0.75-at.% Gd), $dT_{\max,H}/dH = 0.14 \times 10^{-3}$ K/Oe, yielding $g_{\text{eff}} = 2.1$, i.e., a small enhancement of the moment which is hardly outside experimental error.[49] (See Sec. VIII for a comparison with EPR data.) Our analysis of the field dependence of the specific heat is thus consistent with the T_C ratio (Sec. V) in predicting a small enhancement of the moment of Gd in Pd.

TABLE V. Pd(Mn) data obtained from the specific heat (Ref. 16). T_C was identified with the temperature of the specific heat maximum. For all alloys the average $g_{\text{eff}} = 2.9$ was used to obtain γ from $H_m(0)$.

Concentration (at.% Mn)	T_C (K)	$H_m(0)$ (kOe)	γ (10^3 g/emu)
0.08	•••	3.2	10.5
0.19	0.49	4.5	6.2
0.54	1.93	8.7	4.2
1.35	4.50	20	3.9
2.45	5.75	•••	•••

VII. FERROMAGNETIC PROPERTIES

A. Curie temperatures; molecular-field constants

As observed in the specific-heat data,[16] the magnetic transition of dilute Pd(Mn) alloys is unusually sharp compared to Pd(Fe), Pd(Co), or other dilute magnetic alloys. The anomaly is cusp shaped, which is reminiscent of MFM predictions below T_C. However, more than 20% of the entropy of the transition is gained above T_C, which is not expected from the MFM.

Discrepancies have been noted in the literature between Curie temperatures obtained from specific heat, magnetization, and resistivity data for dilute Pd(Fe) and Pd(Co) alloys. Here we will show that such discrepancies do not occur in Pd(Mn) and that the magnetic transition is about as sharp as the specific-heat cusp.

In Fig. 10 we compare low-field magnetization data of Pd(1.35-at.% ZMn) with Pd(0.24-at.% Co). The samples were cut from the specific-heat specimens of Refs. 16 and 34 with $T_C = 4.54$ K for Pd(1.35-at.% Mn)[16] and $T_C = 4.16$ K for Pd(0.24-at.% Co).[34] No magnetic hysteresis was observed in any of our Pd(Mn) alloys (i.e., the width of the hysteresis loop was less than 0.5 Oe). Below the "kink" [Fig. 10(a)] the magnetization is proportional to the applied field and the inverse susceptibility below T_C is independent of the temperature and equal to the demagnetizing factor ($N = \frac{4}{3}\pi$) within experimental error. In contrast, hysteresis was observed in the Pd(0.24-at.% Co) sample over a wide temperature range about "T_C." Here T_C was determined from a fit of a model calculation to specific-heat data,[34] and is close to the temperature of the specific-heat maximum. Evidence of hysteresis remained up to 20 K. It should be noted that the Pd(0.24-at.% Co) alloy was homogenized at 1000 °C for 48 h. A Pd(0.2-at.% Co) alloy, rapidly quenched from the melt, showed a reduction by a factor of ~4 in coercive field at 4.2 K.

In Fig. 11 the magnetization data on Pd(1.35-at.% Mn) close to T_C are plotted in the usual form of σ^2 vs H_i/σ, where H_i is the applied field minus the demagnetizing field $N\sigma$. In such a plot T_C is identified with the isotherm that passes through the origin. From Fig. 11 we thus conclude that $4.533 < T_C < 4.588$ K. A more precise value for T_C can be found when the inverse susceptibility above T_C [i.e., $(H_i/\sigma)_0$ at $\sigma = 0$] is plotted versus the temperature and extrapolated to $(H_i/\sigma)_0 = 0$. The experimental points then lie on a strongly curved line, which makes extrapolation difficult. It is easier to determine a constant γ_+ such that when the points $(H_i/\sigma)_0^{1/\gamma_+}$ are plotted versus temperature they lie on a straight line.[50] This procedure yields $T_C = 4.540 \pm 0.005$ K for Pd(1.35-at.% Mn) in excellent agreement with the specific-heat value of[16] T_C (Table V). The constant γ_+, the critical exponent for the susceptibility above T_C,

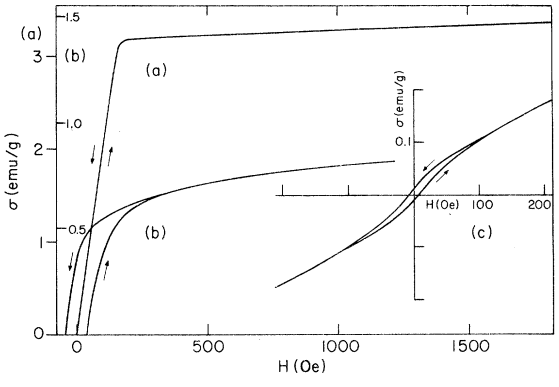

FIG. 10. Comparison of magnetization data of Pd(Mn) and Pd(Co) alloys: (a) Magnetization versus applied field of Pd(1.35-at.% Mn) at $T = 1.3$ K (spherical sample). Up and down sweep data are coincident. The full hysteresis "loop" was taken, but only the positive part is shown. (b) Magnetization versus applied field of Pd(0.24-at.% Co) at $T = 1.3$ K (cylindrical sample). The full loop was taken, but only the positive part is shown. (c) Magnetization of Pd(0.24-at.% Co) at $T = 20$ K.

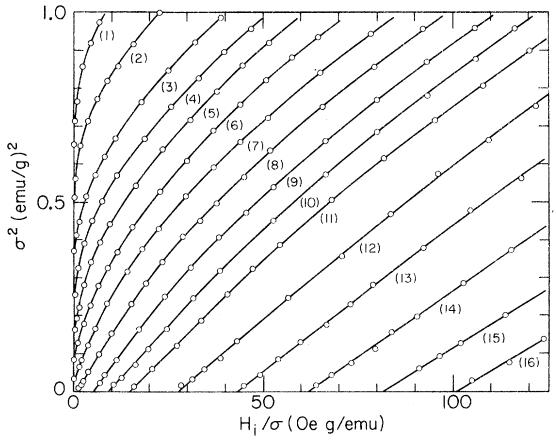

FIG. 11. Magnetization isotherms of Pd(1.35-at.% Mn) close to T_C: (1) $T = 4.336$ K, (2) $T = 4.384$ K, (3) $T = 4.433$ K, (4) $T = 4.459$ K, (5) $T = 4.483$ K, (6) $T = 4.507$ K, (7) $T = 4.533$ K, (8) $T = 4.558$ K, (9) $T = 4.585$ K, (10) $T = 4.613$ K, (11) $T = 4.640$ K, (12) $T = 4.690$ K, (13) $T = 4.735$ K, (14) $T = 4.784$ K, (15) $T = 4.834$ K, (16) $T = 4.882$ K.

would then be $\gamma_+ = 1.53$. (See also Sec. VII B.) Because of the strong curvature of the isotherms in Fig. 11 a reliable value for T_C can be determined only when data are obtained at very small internal fields H_i. Furthermore, the procedure is only meaningful if a Curie temperature does indeed exist, i.e., a temperature at which the susceptibility diverges and a spontaneous magnetization appears. The kink in Fig. 10(a) indicates that below T_C a well defined spontaneous magnetization (i.e., σ at $H - N\sigma = 0$) exists which according to Fig. 11 disappears at a well-defined temperature. For comparison we did some brief measurements on Pd(5-at.% Gd), which is ferromagnetic with $T_C \approx 3$ K. No hysteresis was found, but neither was there a "kink" in the magnetization curve below T_C. Instead, as in Pd(Co), a gradual decrease of $d\sigma/dH$ with increasing field was observed and the specific-heat anomaly was not sharp either. According to the preceding discussion, T_C values obtained from plots of σ^2 vs H_i/σ for dilute Pd alloys with Fe, Co, or Gd must be considered with some caution [cf. also the remarks on Pd(Gd) in Sec. V].

The Curie temperatures are listed in Table VI. These were obtained for some of our alloys using isotherm plots such as those in Fig. 11. Also included are the Curie-Weiss temperatures. Almost all T_C and Θ values for Pd(Mn) up to 4-at.% Mn that have been published so far are presented in Fig. 12. The Θ values from the various sources are in good agreement with each other. The same is true for T_C, obtained from various physical properties (except two points from Ref. 14). As usual, Θ was greater than T_C, indicating that the MFM does not describe the ordering process very well. The initial concentration dependence of T_C is $T_C \sim c^m$, with $m > 1$. From Table VI it appears that Θ varies similarly as c^m, since Θ/c' increases initially with concentration. Around 1-at.%, $m \approx 1$. This behavior can be qualitatively understood when the radial dependence of the matrix polarization is taken into account.[52] This radial dependence may also explain the rapid broadening of the magnetic transition upon progressive dilution of Pd(Mn) alloys below about 0.5-at.% Mn, reflecting a changeover from long-range ferromagnetic order to an ordered state of more short-range character.

It is interesting to compare Fig. 12 with Fig. 6 of Ref. 34 which shows the Curie temperatures of dilute Pd(Co) alloys. The values of Θ and T_C for the two alloy systems [and also Pd(Fe)] appear to scale up to 1-at.% solute concentration (see also Ref. 52). This suggests that one should compare alloys with the *same solute concentration* instead of the same T_C and that the magnetic transition of Pd(1-at.% Fe) and Pd(1-at.% Co) may be as sharp as that of Pd(1-at.% Mn). The latter system may then not be as unique as it seemed to be at first sight. Resistivity data[54] do indeed confirm such an increasing sharpness of the magnetic transition in Pd(Fe). It would be interesting to study the specific heat of Pd(Fe) and Pd(Co) alloys with 1-at.% or higher solute concentration, although the large lattice specific heat will probably inhibit the determination of the solute contribution.

Beyond 1-at.% Mn, T_C and Θ tend to flatten off as a function of concentration. At about 2.5-at.% Mn, Θ attains a maximum (T_C values are not

TABLE VI. Curie-Weiss temperatures Θ and Curie temperatures T_C of Pd(Mn) alloys obtained from, respectively, the low-field susceptibility (Table III) and from isotherms such as those shown in Fig. 11. The trend of Θ/c' and T_C/c' does not change when c' is replaced by c. According to Sec. IV B (Table IV), c' is thought to be more accurate than c. The uncertainties of T_C are mainly determined by the temperature intervals of the isotherms, except for Pd(1.35-at.% Mn), where rounding causes the error.

Alloy (at.% Mn)	Θ (K)	Θ/c' (K/at.% Mn)	T_C (K)	T_C/c' (K/at.% Mn)
0.05	0.180	4.12	...	...
0.054	0.241	4.53	...	...
0.08	0.387	4.89	...	...
0.23	1.334	5.77	...	...
0.49	2.66	5.92	1.55 ± 0.05	3.44
0.96	4.56	4.79	3.45 ± 0.05	3.62
1.35	5.48	4.25	4.540 ± 0.005	3.52
2.45	7.12	3.04	6.14 ± 0.02	2.62

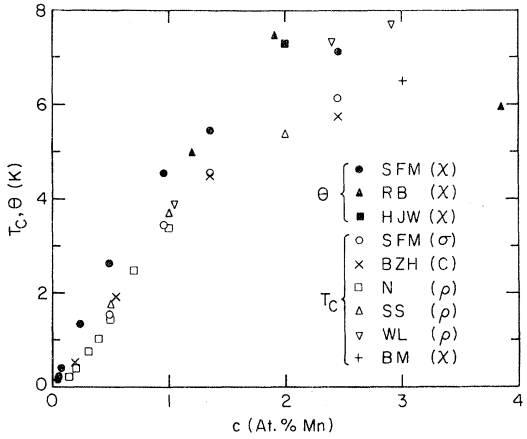

FIG. 12. Comparison of Curie-Weiss temperatures θ and Curie temperatures T_C of Pd(Mn) alloys reported from various sources. SFM: present work, susceptibility and magnetization; RB: Ref. 32, susceptibility; HJW: Williams quoted in Ref. 12, susceptibility; BZH: Ref. 16, specific heat; N: Refs. 52 and 53, resistivity; SS: Ref. 12, resistivity; WL: Ref. 14, resistivity; BM: Ref. 51, susceptibility.

available above 2.9-at.% Mn) and eventually becomes negative.[32] This maximum as well as the trend of Θ/c' and T_C/c' in Table VI reflects the increasing importance of direct AF interactions between neighboring Mn atoms, which were mentioned before in Secs. III B and V.

The trend of the molecular-field constant γ (Table III) as a function of Mn concentration is similar to that of Θ. According to the MFM, $\gamma = \Theta/C$. Because p_{eff} (and therefore C) decreases only slowly with increasing concentration, the trend of γ is determined mainly by the variation of Θ. Less weight should be given to the γ values obtained from the specific heat (Table V), because these depend on the analyzed concentration (in contrast to the γ values of Table III) and were obtained in a temperature region closer to T_C so that they are more sensitive to the deficiencies of the MFM.

B. Spontaneous magnetization and spin-wave stiffness constant

From Fig. 11 one can also obtain the spontaneous magnetization. A common method is to draw lines of constant σ_s and plot the points $(H_i/\sigma,\ T)$ obtained from the intersections with the isotherms. The temperature corresponding to a particular value of σ_s is found from extrapolation to $H_i/\sigma = 0$. Again, it may be easier to plot $(H_i/\sigma)^{1/\gamma+}$ vs T (cf. also Sec. VII B). In this way we determined values of σ_s close to T_C for the three most concentrated Pd(Mn) alloys. Below $T = 0.9T_C$ it is more convenient to use the "kink" [Fig. 10(a)] as a measure of σ_s. For a magnetic transition where hysteresis, anisotropy, and other rounding effects are negligible, $d\sigma/dH$ should be discontinuous and the determination of σ_s would be unambiguous. The present Pd(Mn) alloys show some rounding (see also below) and we arbitrarily identified σ_s with the point at the kink where $d\sigma/dH$ is approximately $\frac{1}{3}$ of the initial slope, i.e., $1/3N$, where N is the demagnetizing factor. In the region where both methods were employed, the σ_s values differed *at most* by 3% which was adequate for our purpose.

Boerstoel[16] has attempted to determine critical exponents for the specific heat of some Pd(Mn) alloys near T_C. The fact that some rounding of the transition is observed was assumed to be due to the statistical distribution of Mn atoms in the Pd lattice and was accounted for by including a Gaussian distribution of T_C values in the fitting procedure by which the critical exponents were obtained from experimental data. It was found that $\alpha_- < -1$, but α_- approaches the value -1 with increasing Mn concentration (for definitions see Ref. 16). In view of the long-range matrix polarization one is tempted to think of an approach to molecular-field behavior ($\alpha_- = -1$), but apart from the results discussed in Sec. VI there is no further support for that assumption.

If a description of the Pd(Mn) transition by means of critical exponents makes sense, the exponent β for the spontaneous magnetization should approach $\beta = \frac{1}{2}$ (such as α_- approaches the value -1). In this case it is very difficult to account for the observed rounding, because in addition T, H_i is involved as a parameter in the determination of σ_s. Rounding effects were therefore ignored. From the data shown in Fig. 11 we find for Pd(1.35-at.% Mn): $\beta \approx 0.60$ and $\gamma_+ \approx 1.53$. Both values are unusually large, which is to be expected when rounding is neglected. Therefore, if critical exponents can be defined at all for the magnetic transition of dilute Pd(Mn) alloys they do not seem to be useful here.

The data further below T_C permit some interesting conclusions to be drawn. In Fig. 13(a) σ_s is plotted as a function of T/T_C for three Pd(Mn) alloys and is compared with the MFM using the average moment of Mn in these three alloys (from Table IV the average of $g'S = 6.96\mu_B$/Mn). The spontaneous moment per Mn atom at $T = 0$ is

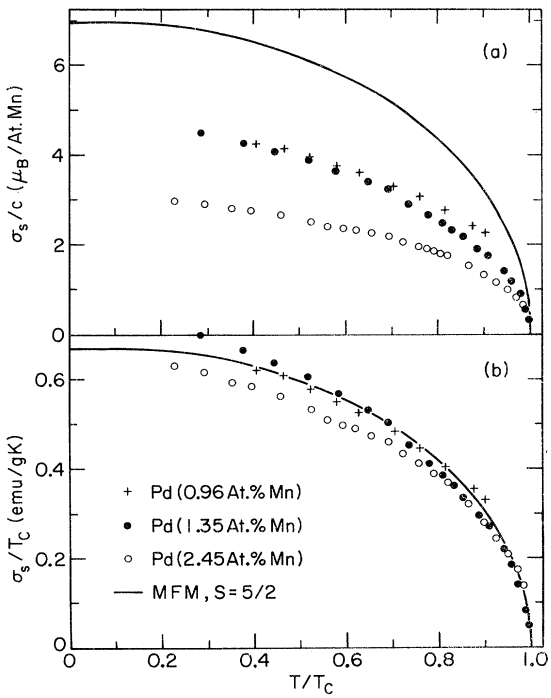

FIG. 13. Spontaneous magnetization versus temperature: (a) Spontaneous magnetization σ_s in μ_B per solute atom versus T/T_C for three Pd(Mn) alloys. The solid line represents the molecular-field model for $S = \frac{5}{2}$ using the average saturation moment per atom of the three alloys; (b) σ_s/T_C. The solid line represents the molecular-field model scaled to $\sigma_s/T_C = 0.67$ emu/g K at $T = 0$.

evidently considerably smaller than the saturation moment, and decreases with increasing Mn concentration. This is caused by antiferromagnetically interacting (AF) Mn atoms which are not, or only weakly, polarized by the ferromagnetic exchange field [the maximum exchange field $\gamma\sigma(T=0) \approx 20$ kOe for both Pd(1.35-at.% Mn) and Pd(2.45-at.% Mn)]. As Fig. 13(b) shows, the data for the various alloys can be brought closer together when σ_s is normalized by T_C. This suggests that in a first approximation the AF Mn atoms may be neglected and an effective concentration of ferromagnetically interacting (F) Mn atoms may be defined, to which T_C and σ_s are proportional. The resistivity data of Williams and Loram[14] support this conjecture. In Table VII the normalized resistivity "step" $[\Delta\rho(T_C) - \Delta\rho(T=0)]/c$ decreases strongly, but $[\Delta\rho(T_C) - \Delta\rho(T=0)]/T_C$ decreases only slightly with increasing Mn content of the alloys.

Using the MFM relationship, $\sigma_0/T_C = 3k_B/\gamma g_{\text{eff}}\mu_B(S+1) = 0.67$ emu/g K (Fig. 13) and $g_{\text{eff}} = 2.78$ (the average of g'_{eff} for the last three alloys of Table IV), we obtain $\gamma = 6.8\times10^3$ Oe g/emu and $T_C = 5.45$ K/at.% Mn. These values are somewhat larger than those given in Table III for the alloys considered in this section, because the former now apply to the F Mn atoms only whereas the latter represent the total effect of both F and AF Mn atoms.

In order to obtain a rough estimate of the number of AF Mn atoms, we assume that a number n exists such that an Mn atom which has no neighbors within a sphere containing n lattice sites interacts ferromagnetically with others of the same kind. If a Mn atom does have one or more neighbors within that region it interacts antiferromagnetically with these neighbors, and does not contribute to σ_s or to T_C (n might be called a coordination number for AF interactions). The ratio of the number of F Mn atoms to the total number of Mn atoms is then $(1-c)^n$. Values of n obtained in this way, using $T_C = 5.45$ K/at.% found above for the F Mn atoms, are given in Table VIII. It appears that Mn atoms that are more than a next-nearest-neighbor distance apart may still interact antiferromagnetically. The decrease of n with increasing c should not be taken seriously, in view of the simplifying assumptions underlying the estimates. A more detailed discussion will be presented in Sec. VII C.

The spontaneous magnetization of two alloys is plotted as a function of $(T/T_C)^{3/2}$ in Fig. 14. We do not consider this figure a proof of the $T^{3/2}$ dependence of σ_s at small T/T_C because the precision of the data is insufficient and they do not extend to low enough temperature.[55] Instead, we will take the $T^{3/2}$ dependence for granted, in order to determine values for the acoustic spin-wave stiffness constant D. The spontaneous magnetization is assumed to vary according to the well-known spin-wave formula (see, e.g., Ref. 56)

$$\sigma_s(T) = \sigma_s(0) - (2.612 g_{\text{eff}}\mu_B c/8\pi^{3/2}\rho)(k_B T/D)^{3/2}, \tag{12}$$

where ρ is the density of the alloy. Values for D obtained from Fig. 14 and Eq. (12) are given in Table IX. D appears to be proportional to T_C when the analyzed Mn concentration is multiplied by the ratio of F Mn atoms to the total number of Mn atoms (see the discussion of Table VIII) and this D value is in very good agreement with the experimental result $D \approx 0.7$ Å^2 K of Williams *et al.*,[15,56] which was obtained from electrical resistivity data. These authors eliminated the Mn concentration from the formula for the $T^{3/2}$ term of the resistivity using $\Delta\rho(T_C) - \Delta\rho(0)$. We have seen (Table VII) that $\Delta\rho(T_C) - \Delta\rho(0)$ is a good measure of the number of F Mn atoms so that the agreement between Williams's and our results can be taken as a support for the preceding analysis.

Theoretical expressions for the spin-wave stiffness constant of giant-moment alloys have been derived by Doniach and Wohlfarth[30] and by Cole and Turner,[57] and were compared with experiments by Williams and Loram.[56] We will compare our Pd(Mn) data with the Doniach-Wohlfarth formula

$$D = 2cS\hbar^2(\lambda\chi_0)^2/(1+\lambda\chi_0)27z\,m_d^*, \tag{13}$$

TABLE VII. Pd(Mn) resistivity data of Williams and Loram (Ref. 14).

c (at.% Mn)	$[\Delta\rho(T_C) - \Delta\rho(T=0)]/c$ ($\mu\Omega$ cm/at.%)	$[\Delta\rho(T_C) - \Delta\rho(T=0)]/T_C$ ($\mu\Omega$ cm/K)
1.05	0.097	0.026
2.40	0.078	0.025
2.91	0.061	0.023

TABLE VIII. Estimate of the number of antiferromagnetically interacting Mn atoms.

Alloy (at.% Mn)	T_C (expt) (K)	$5.45c$ (K/at.%)	Ratio $= (1-c)^n$	n
0.96	3.45	5.23	0.66	43
1.35	4.54	7.36	0.62	36
2.45	6.14	13.4	0.46	31

where z is the number of d holes per atom of the matrix and m_d^* is a d-band effective mass. When the experimental value is substituted for $\lambda\chi_0 = (\frac{1}{2}g'_{\rm eff}) - 1$ (Table IV) and the analyzed concentration is corrected for the AF Mn atoms (Table VIII), one obtains $D = 11(m_e/m_d^*)T_C$ Å^2 K. This agrees with experiment if $m_d^* \approx 15 m_e$ which is about the same value as used by Williams and Loram.[56] Alternatively, $\lambda\chi_0$ and c may be eliminated from Eq. (13) using Eq. (9) which yields

$$D/k_B T_C = 2\chi_0 \hbar^2/N_l(S+1)g_{\rm eff}\, g_0 \mu_B^2 z\, m_d^*, \qquad (13a)$$

where N_l is the number of lattice sites per gram. Equation (13a) agrees with the experimental data if $m_d^* \approx 6 m_e$. The discussion in Eq. (9) in Sec. V also applies here. We thus arrive at the same conclusion as Williams and Loram, namely, that theory and experiment on D agree within a factor 2 or 3. This is not unreasonable in view of the approximations involved, viz., use of the MFM for the ferromagnetic interaction and the effective-mass approximation for the d-hole energy spectrum. More importantly, the values for D obtained experimentally from electrical resistivity and spontaneous magnetization data agree very well. However, some caution should be exercised, because the contribution of the AF Mn atoms to the electrical resistivity and spontaneous magnetization is probably not negligible. This is apparent in the specific-heat data,[16] which do not vary as $T^{3/2}$ in the temperature region where the other properties do vary in this manner.

Williams *et al.*[15] have suggested the occurrence of optical spin waves in dilute ferromagnetic Pd(Mn). This suggestion was based on Doniach

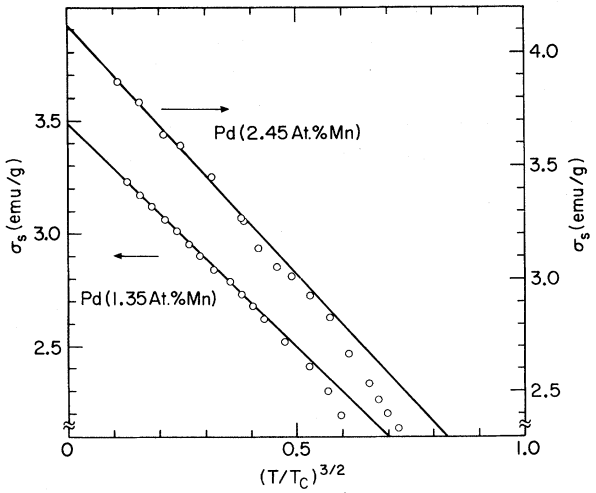

FIG. 14. Spontaneous magnetization of two Pd(Mn) alloys versus $(T/T_C)^{3/2}$.

TABLE IX. Experimental spin-wave stiffness constant D for two Pd(Mn) alloys. The values D (corr.) were obtained after multiplication of the concentration by the ratio $T_C/5.45c$ (see Table VIII). For $g_{\rm eff}$ the values $g'_{\rm eff}$ in Table IV were used.

Alloy (at.% Mn)	$d\sigma_s/d(T/T_C)^{3/2}$ (emu/g)	D (Å^{2}K)	D (corr) (Å^{2}K)
1.35	−1.98	$0.92T_C$	$0.67T_C$
2.45	−2.21	$1.21T_C$	$0.72T_C$

and Wohlfarth's expression for the energy of an optical mode at zero wave vector, which can be written

$$E_{\rm opt} = cJ\mu/\mu_B = cN_l\lambda(1+\lambda\chi_0)Sg_0^2\mu_B^2, \qquad (14)$$

where μ is the giant moment (J is defined in Ref. 30). Equation (14) yields $E_{\rm opt} \approx 37$ K/at.% Mn. This is considerably larger than the value proposed by Williams *et al.*[15] because the values for J and μ used by them are too small. It seems to us, therefore, that optical spin waves play a negligible role in the Pd(Mn) system.

C. Antiferromagnetic interactions

In previous sections the assumption of antiferromagnetic interactions between near-neighbor Mn atoms was employed to explain the relatively small spontaneous magnetization and the high fields required for saturation. Also, an estimate was made of the range of these AF interactions. In the present section we discuss a simple model to fit the high-field magnetization of two Pd(Mn) alloys. From the parameters of this model, estimates will be obtained for the magnitude of the AF interaction energy and for the number of Mn atoms involved.

We assume that all Mn atoms in the alloy have the same moment (i.e., cause the same matrix polarization) and that the resulting ferromagnetic interaction is described by a single molecular-field constant γ_F. The long range of the matrix polarization and the discussion in previous sections may to a certain extent justify the use of γ_F. In addition, Mn atoms within a certain distance are assumed to interact antiferromagnetically. This interaction is assumed to be a pair interaction, and to be independent of their mutual distance and of the distance of other Mn atoms. It is also described by a molecular-field constant γ_A. Because the AF interaction is short range, the use of γ_A has no particular justification but is a crude approximation. The magnetization of Mn atoms interacting ferromagnetically only is σ_1, with saturation magnetization σ_{10}. The remaining Mn atoms have magnetization σ_2 with saturation

value σ_{20}. The following equations then hold:

$$\sigma_1 = \sigma_{10} B_S \left(\frac{g_{\text{eff}} \mu_B S}{k_B T} (H + \gamma_F \sigma_1 + \gamma_F \sigma_2) \right) \tag{15}$$

and

$$\sigma_2 = \sigma_{20} B_S \left(\frac{g_{\text{eff}} \mu_B S}{k_B T} (H + \gamma_F \sigma_1 + \gamma_F \sigma_2 - \gamma_A \sigma_2) \right), \tag{16}$$

where B_S is the Brillouin function. One might argue that for the AF coupling the unenhanced g_0 should be used, rather than g_{eff}. However, an analysis along the lines of Eqs. (5)–(8), including AF coupling, shows that Eq. (16) is correct. It should be noted that, although the AF exchange field $\gamma_A \sigma_2$ contains the bulk magnetization σ_2 (for convenience) it represents the effect of one Mn atom on one neighbor.

We are interested in the magnetization at high fields where σ_1 is nearly saturated (see the discussion below, and Table X). Equation (15) then reads $\sigma_1 = \sigma_{10}$ and Eq. (16) becomes

$$\sigma_2 = \sigma_{20} B_S \left(\frac{g_{\text{eff}} \mu_B S}{k_B T} [H + \gamma_F \sigma_{10} + (\gamma_F - \gamma_A) \sigma_2] \right), \tag{16a}$$

which is easily solved if the constants are known. Equation (16a) will be fitted to the magnetization of Pd(1.35-at.% Mn) and Pd(2.45-at.% Mn) at $T = 4.2$ K and in applied fields above 40 kOe (to satisfy $\sigma_1 = \sigma_{10}$). The total magnetization at $H = 0$ and $T = 0$ [$\sigma(0, 0)$] is obtained by extrapolation in Fig. 14, giving the equation $\sigma(0, 0) = \sigma_{10} + \sigma_2(0, 0)$. A second equation for σ_{10} and $\sigma_2(0, 0)$ in terms of γ_F and γ_A is then found from the argument of B_S in Eq. (16a), i.e., $\gamma_F \sigma_{10} + (\gamma_F - \gamma_A)\sigma_2 = 0$ at $H = 0$ and $T = 0$. From σ_0 ($= \sigma_0'$, Table IV) we get $\sigma_{20} = \sigma_0 - \sigma_{10}$, which leaves two unknowns, γ_F and γ_A. From Eqs. (15) and (16) one easily derives an expression for the Curie temperature, i.e., the temperature T_C at which the susceptibility

$$\chi = \sigma_0 Q / [1 - \sigma_0 Q \gamma_F + \sigma_{20}^2 Q \gamma_A / (\sigma_0 + \sigma_{10} \sigma_{20} Q \gamma_A)] \tag{17}$$

diverges [$Q = g_{\text{eff}} \mu_B (S + 1)/3 k_B T$]. T_C is largely determined by γ_F. Values for γ_F and γ_A were chosen so that T_C was equal to the measured Curie temperature. By trial and error these values were changed (keeping T_C fixed) until the computed magnetization $\sigma = \sigma_{10} + \sigma_2$ best fitted the experimental data. The results are shown in Fig. 15. For Pd(1.35-at.% Mn) the deviation between the model and the data is less than 1% of σ. Around $H = 50$ kOe the model magnetization is smaller than the data, contrary to what we expect because of the approximation $\sigma_1 = \sigma_{10}$. This suggests that not all AF interactions have the same magnitude, but that values smaller than the average represented by γ_F occur. This is more obvious in the Pd(2.45-at.% Mn) data. Here the fit is not very good. It seems that at 210 kOe the solute magnetization was not fully saturated so that the parameters used (viz., σ_0, g_{eff}, etc.) may have been slightly in error. It is clear that AF interactions both weaker and stronger than the value represented by γ_A do occur.

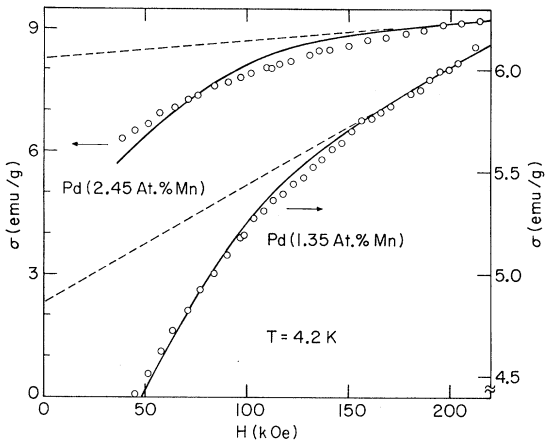

FIG. 15. Magnetization of two Pd(Mn) alloys as a function of applied field at $T = 4.2$ K. Solid lines: model calculation as discussed in the text. Dashed lines: high field slopes from Curie-Weiss fits of the susceptibility data.

The model parameters for the two alloys are listed in Table X. The molecular-field constant γ_F of Pd(1.35-at.% Mn) does not differ much from the one in Table III, but γ_F of Pd(2.45-at.% Mn) is considerably larger. This is probably a continuation of the increase of γ_F for the alloys up to 0.49-at.% Mn, which in Table III was masked by the large number of AF solute atoms. From the AF exchange field $\gamma_A \sigma_{20}$ it follows that the AF interaction energy is $E_{\text{int}} \approx \gamma_A \sigma_{20} g_{\text{eff}} \mu_B S = 7.7 \times 10^{-15}$ erg (≈ 55 K) for both alloys. Williams *et al.*[15] have

TABLE X. Model parameters used in Eq. (16a) to obtain the solid lines in Fig. 15. χ_0 and g_{eff} were taken from Tables III and IV, respectively. n is the "coordination number" for antiferromagnetic interactions (see text).

Parameter	1.35-at.% Mn	2.45-at.% Mn
g_{eff}	2.86	2.65
χ_0(emu/g)	5.75×10^{-6}	4.36×10^{-6}
σ_{10}(emu/g)	3.15	2.86
σ_{20}(emu/g)	1.71	5.40
$\sigma(0, 0)$ (emu/g)	3.48	4.12
γ_F(Oe-g/emu)	5.87×10^3	7.73×10^3
$\gamma_A \sigma_{20}$(kOe)	105	137
n	32	43

estimated E_{int} on the basis of Caroli's double resonance mechanism[59] and obtained $E_{int} \approx 15$ K for nearest neighbors, consistent with their experimental result.[58] However, the theoretical value is extremely sensitive to the parameters (because $k_F R$ is large) and could easily be a factor of 2 larger. According to the double resonance mechanism, interaction with second- and third-nearest neighbors may also be of AF sign (though weaker). Moriya[9] has shown that covalent admixture may also cause AF coupling between nearest-neighbor Mn atoms, but the magnitude of the coupling is difficult to estimate.

One may wonder how much the AF coupling would affect the measured spin value. This can be estimated as follows. If the interaction energy has the form $E = -J\vec{S}_1 \cdot \vec{S}_2$, where $\vec{S}_1$ and $\vec{S}_2$ are Mn spin vectors, this energy is proportional to the cosine of the angle between the spins. The specific heat (Schottky anomaly) and entropy are then easily calculated. Measurements were performed[16] up to 30 K where, according to this model (if $S = \frac{5}{2}$ and $E_{int} = 55$ K), 70% of the entropy is recovered. In the worst case [Pd(2.45-at.% Mn)], about 60% of the Mn atoms interact AF, so that 18% of the entropy would be lacking at 30 K. Considering that the entropy data are extrapolated from plots of entropy versus T^{-2}, at least two-thirds of this remaining entropy is probably also recovered. If indeed one obtains 94% of the total entropy, the experimental spin value would be low by 11% which is consistent with the data.[16]

Referring to Sec. VII B we now redefine n such that a Mn atom that has no neighbors within a sphere containing n lattice sites interacts ferromagnetically with all others, whereas a Mn atom that does have one or more neighbors within that range, in addition, interacts antiferromagnetically with these neighbors. It follows that $(1-c)^n = \sigma_{10}/\sigma_0$ and n thus obtained is listed in Table X. As in Sec. VII B we conclude that AF interactions extend to third-nearest neighbors. One might guess that n would be close to either the number of first neighbors (12), the sum of first and second neighbors (18), or the sum of first, second, and third neighbors (42). The fact that $18 < n < 42$ in one case, and that n seems to increase with c must be attributed to the simplicity of the model. The values of n might be explained if nearest-neighbor Mn atoms interact AF, second neighbors F, and third neighbors AF. Williams *et al.*[15] have estimated the fraction of F and AF Mn atoms in a Pd(2.91-at.% Mn) alloy from magnetoresistivity data. In zero applied field they found 0.955-at.% F and 1.955-at.% AF Mn atoms, so that $n \approx 38$, in good agreement with the results in Table X (see also Table VIII).

Taking fixed values for n, γ_F, and $\gamma_A \sigma_{20}$, the model discussed in this section can be used to compute T_C as a function of Mn concentration. It turns out that T_C increases monotonically, instead of passing through a maximum (Fig. 12; see also Fig. 6 of Ref. 16). This indicates that the AF nearest-neighbor interaction is larger than the average value for n-neighbor sites obtained from the model, and becomes more dominant as the number of nearest-neighbor pairs increases. It is also possible that the strength of the AF coupling depends on the presence of other Mn atoms. With the large value of n (≈ 38), at $c = 2$ at.% more than 15% of the Mn atoms occur in triples or larger groups. Finally, the ferromagnetic exchange constant γ_F will decrease when the ratio of F to AF Mn atoms becomes small.

When χ^{-1} [Eq. (16)] is plotted versus T, the resulting curve is concave toward the T axis (as for a ferrimagnet), so that $\Theta < T_C$, in contrast with experiment. It should be noted, however, that the minimum temperature of the range of fit (Table III) approaches the value Θ as c increases. This may be the result of the AF interactions.

Although the foregoing remarks demonstrate some limitations of the model, it nevertheless gives a satisfactory account of the high-field magnetization and provides some insight into the interactions in Pd(Mn) alloys.

VIII. REMARKS ON RELATED EXPERIMENTS

We have shown that, in order to consistently describe the low-field susceptibility, magnetization and specific heat of dilute paramagnetic Pd(Mn) alloys, the "giant" moment of Mn must be assigned a "normal" spin $S = \frac{5}{2}$ and a "giant" effective g value $g_{eff} \approx 3$. One may wonder how this result compares with EPR data. Cottet[60] has measured the EPR of Pd(Mn) alloys (for $c \geq 0.23$-at.% Mn) and found $g = 2.2$ in the limit of low concentration. This is considerably smaller than g_{eff}, but the two values are not directly comparable. In EPR, unlike static experiments, relaxation effects play an important role. Taking as a guide the phenomenological theory of Hasegawa[61] one expects a large g shift (consistent with $g_{eff} \approx 3$ for Mn in Pd) when the band-electron-spin–lattice relaxation time is short compared to the band-electron–local-moment relaxation time. Since the observed g shift is relatively small one might think that the spin-lattice relaxation time is long. However, according to Coles *et al.*[62] the resonance of Mn in Pd is not bottlenecked, so that it is rather difficult to reconcile the "static" with the "dynamic" g value. A similar and even more serious problem occurs with Gd in Pd. Here a

small enhancement of the moment of Gd is inferred from specific-heat and magnetization data (cf. Secs. V and VI) so that $g_{\text{eff}} > 2$, whereas the observed EPR g shift is negative.[11,63] The discussion of these problems is beyond the scope of our paper. We wish to emphasize, however, that within the context of static experiments as discussed in the foregoing sections all data are consistent with a large $g_{\text{eff}} = \mu/S$.

EPR measurements on single-crystal dilute Pd(Mn) alloys revealed no anisotropy.[64] Neither did Nieuwenhuys[65] find any anisotropy in the specific heat of single-crystal Pd(0.1-at.% Fe) and Pd(0.1-at.% Co) alloys as a function of applied magnetic field.

We finally wish to point out a certain similarity between Pd(Mn) and $(Ge_{1-x}Mn_x)Te$.[66] The latter system is also ferromagnetic, with $T_C \approx 4$ K/at.% Mn, almost equal to that of Pd(Mn). The interactions are carried by the conduction electrons through the Ruderman-Kittle-Kasuya-Yosida (RKKY) polarization. The ferromagnetic sign of the interaction seems to occur because k_F is small so that the first zero of the RKKY oscillations occurs far away from the solute atom. It would be interesting to measure, e.g., the specific heat of $(Ge_{1-x}Mn_x)Te$ to see if a similar cusp occurs as in Pd(Mn). A giant moment has not been observed for $(Ge_{1-x}Mn_x)Te$ and is not expected, for the following reason. If we arbitrarily assume that the susceptibility of the carriers in $(Ge_{1-x}Mn_x)Te$ is $10^{-2}\chi_{Pd}$ then, using Eq. (9) and the fact that the Curie temperatures are equal, we see that $\lambda\chi_0$ should be ten times smaller than in Pd(Mn) so that the moment would be only slightly enhanced. The value of λ yields a value for the exchange interaction, using Eq. (2.3) of Ref. 29, $2J = \lambda N g_0^2 \mu_B^2 \approx 1$ eV, which is of the same order of magnitude as reported by Cochrane *et al.*[66]

ACKNOWLEDGMENTS

Thanks are due to Dr. P. F. de Chatel and Dr. G. J. Nieuwenhuys for careful reading of the manuscript and fruitful discussions, and to Dr. G. J. van den Berg for his interest in this work. Thanks are also due to Dr. B. Knook and his coworkers for their care in preparing the alloys and to M. Otten for performing the chemical analyses. We acknowledge the technical assistance of W. G. Fisher and A. Djiauw and the efforts of E. J. Alexander in spark cutting some Pd(Mn) spheres. One of us (W.M.S.) thanks the staff of the Francis Bitter National Magnet Laboratory for their hospitality and support during his Fellowship.

---

*Work at the Francis Bitter National Magnet Laboratory supported by a NATO Science Fellowship, awarded by the "Netherlands Organization for the Advancement of Pure Research" (Z.W.O).

†Work at the Kamerlingh Onnes Laboratorium partly supported by the "Foundation for Fundamental Research on Matter" (F.O.M.).

‡Supported by the National Science Foundation.

§Present address: Fysisch Laboratorium, Rotterdam Radiotherapeutisch Instituut, P. O. Box 5201, Rotterdam, Netherlands.

[1]R. M. Bozorth, P. A. Wolff, D. D. Davis, V. B. Compton, and J. H. Wernick, Phys. Rev. 122, 1157 (1961).

[2]G. Chouteau and R. Tournier, J. Phys. 32, C1-1002 (1971).

[3]Sometimes superparamagnetic clusters, such as occur in Cu(Ni) or Rh(Ni) alloys, have been called giant moment. We will reserve this term for an impurity with its surrounding positive host polarization, irrespective of its magnitude.

[4]J. Crangle and W. R. Scott, J. Appl. Phys. 36, 921 (1965).

[5]F. R. deBoer, C. J. Schinkel, J. Biesterbos, and S. Proost, J. Appl. Phys. 40, 1049 (1969); M. S. Schalkwijk, P. E. Brommer, G. J. Cock, and C. J. Schinkel, J. Phys. 32, C1-997 (1971); P. R. Liddel and R. Street, J. Phys. F 3, 1648 (1973).

[6]W. M. Star, S. Foner, and E. J. McNiff, Jr., Phys. Lett. A 39, 189 (1972).

[7]W. M. Star, E. de Vroede, and C. vanBaarle, Physica 59, 128 (1972).

[8]P. Lederer and D. L. Mills, Phys. Rev. 165, 837 (1968).

[9]T. Moriya, in *Proceedings of the International School of Physics "Enrico Fermi," Course XXXVII,* edited by W. Marshall (Academic, New York, 1967).

[10]I. A. Campbell, J. Phys. C 1, 687 (1968).

[11]D. Shaltiel, J. H. Wernick, H. J. Williams, and M. Peter, Phys. Rev. 135, A1346 (1964).

[12]M. P. Sarachik and D. Shaltiel, J. Appl. Phys. 38, 1155 (1967).

[13]H. J. Willaims, as quoted in Ref. 12.

[14]G. Williams and J. W. Loram, Solid State Commun. 7, 1261 (1969).

[15]G. Williams, G. A. Swallow, and J. W. Loram, Phys. Rev. B 7, 257 (1973).

[16]B. M. Boerstoel, J. J. Zwart, and J. Hansen, Physica 57, 397 (1972).

[17]G. J. Nieuwenhuys, B. M. Boerstoel, and W. M. Star, in *Proceedings of the Thirteenth International Conference on Low Temperature Physics, Boulder, 1972,* edited by K. D. Timmerhaus, W. J. O'Sullivan, and E. F. Hammel (Plenum Press, New York, 1974), Vol. 2, p. 510.

[18]FM-1 magnetometer, manufactured by Princeton Applied Research Corp., Princeton, N.J.

[19]N. F. Oliveira, Jr. and S. Foner, Rev. Sci. Instrum. 43, 37 (1972).

[20]W. N. Lawless, Rev. Sci. Instrum. 42, 561 (1971).

[21]L. G. Rubin and W. N. Lawless, Rev. Sci. Instrum. 42, 571 (1971).
[22]Sensor and electronics manufactured by Lake Shore Cryotronics, Inc., 9631 Sandrock Road, Eden, N. Y. 14057.
[23]S. Foner and E. J. McNiff, Jr., Rev. Sci. Instrum. 39, 171 (1968).
[24]H. Danan, A. Herr, and A. J. P. Meyer, J. Appl. Phys. 39, 669 (1968).
[25]It may be argued that $\mu H/k_B T$ at 1.4 K and 150 kOe is larger than at 4.2 K and 210 kOe. However, when $\mu H/k_B T \gg 1$, T is not important, but then what matters is the magnitude of μH compared to other energies, e.g., direct Mn-Mn interactions as discussed later.
[26]S. Foner, R. Doclo, and E. J. McNiff, Jr., J. Appl. Phys. 39, 551 (1968); H. C. Jamieson and F. D. Manchester, J. Phys. F 2, 323 (1972).
[27]D. Gerstenberg, Ann. Phys. 2, 236 (1958).
[28]R. P. Guertin, H. C. Praddaude, S. Foner, E. J. McNiff, Jr., and B. Barsoumian, Phys. Rev. B 7, 274 (1973).
[29]T. Takahashi and M. Shimizu, J. Phys. Soc. Jpn. 20, 26 (1965).
[30]S. Doniach and E. P. Wohlfarth, Proc. R. Soc. A 296, 442 (1967).
[31]The value $\lambda_{Fc}\chi_{Pd} \approx 2$ is based upon a total moment of $10\mu_B$ and an assumed on-site moment of $3\mu_B$, in accordance with $S \approx \frac{3}{2}$ (Ref. 34) and with neutron scattering data (Ref. 35). For further discussion see Sec. V.
[32]J. Rault and J. P. Burger, C. R. Acad. Sci. B 269, 1085 (1969).
[33]For Pd(0.23-at.% Mn), $\Delta\chi_i/\chi_0 = 0.6$ at $T = 50$ K, and $= 0.4$ at $T = 80$ K. For Pd(0.49-at.% Mn), $\Delta\chi_i/\chi_0 \approx 1$ at $T = 50$ K, and ≈ 0.7 at $T = 80$ K. Because the maximum in the matrix susceptibility disappears upon alloying, an upper bound of 50 K seems to be reasonable. Further discussion is given in Sec. IV B.
[34]G. J. Nieuwenhuys, B. M. Boerstoel, J. J. Zwart, H. D. Dokter, and G. J. van den Berg, Physica 62, 278 (1972); also see G. J. Nieuwenhuys, Ph.D. thesis (University of Leiden, 1974) (unpublished).
[35]G. G. Low and T. M. Holden, Proc. Phys. Soc. Lond. 89, 119 (1966).
[36]J. Crangle, Philos. Mag. 5, 335 (1960).
[37]D. J. Kim and B. B. Schwartz, Phys. Rev. Lett. 20, 201 (1968).
[38]A. J. Manuel and M. McDougald, J. Phys. C 3, 147 (1970).
[39]M. P. Maley, R. D. Taylor, and J. L. Thompson, J. Appl. Phys. 38, 1249 (1967).
[40]A. D. C. Grassie, G. A. Swallow, G. Williams, and J. W. Loram, Phys. Rev. B 3, 4154 (1971).
[41]B. M. Boerstoel, J. E. van Dam, and G. J. Nieuwenhuys, in *Proceedings of the NATO Advanced Study Institute, "Magnetism, Current Topics,"* edited by S. Foner (Gordon and Breach, to be published); also, B. M. Boerstoel, Ph.D. thesis (University of Leiden, 1970) (unpublished).
[42]R. P. Guertin and S. Foner, J. Appl. Phys. 41, 917 (1970).
[43]P. W. Bellarby and J. Crangle, J. Phys. C 3, S362 (1970).
[44]J. J. Zwart (Kamerlingh Onnes Laboratory, Leiden) (unpublished data).
[45]J. Crangle, Phys. Rev. Lett. 13, 569 (1964).
[46]This is an assumption, based on the expected ^8S state for Gd. Reliable experimental data for the spin of Gd in Pd are not available. From the entropy, measured on alloys of 3-, 5-, and 7.7-at.% Gd, Bellarby and Crangle (Ref. 43) obtain $S \approx 2.4$. Zwart (Ref. 44) finds $S \approx 2.4$ for Pd(7-at.% Gd), but reports problems with oxidation of Gd and changes in the lattice specific heat. Furthermore, the specific heat appears to be quite sensitive to annealing.
[47]H. C. Praddaude, R. P. Guertin, S. Foner, and E. J. McNiff, Jr., AIP Conf. Proc. 10, 1115 (1973). More recent analysis shows $\simeq 7\mu_B$/Gd atom for all concentrations.
[48]Boerstoel drew a line through the points at $H = 0$ and $2 \leq H/H_m(0) \leq 10$ of his model calculation (Fig. 10 of Ref. 16). Alternatively, a line can be drawn through all points $0.2 \leq H/H_m(0) \leq 10$, excluding $H = 0$. The slope $dT_{\max,H}/dH$ is then nearly equal to that for a spin system without interactions. For $S = \frac{5}{2}$, $dT_{\max,H}/dH = 0.83 g_{\text{eff}}\mu_B/k_B$, yielding $g_{\text{eff}} = 2.7$ instead of $g_{\text{eff}} = 2.9$.
[49]The same remark applies as in Ref. 48. For $S = \frac{7}{2}$, $dT_{\max,H}/dH = 1.025\, g_{\text{eff}}\mu_B/k_B$, yielding $g_{\text{eff}} = 2.0$ instead of $g_{\text{eff}} = 2.1$ for Pd (0.75-at.% Gd).
[50]J. S. Kouvel and M. E. Fisher, Phys. Rev. 136, A1626 (1964).
[51]J. P. Burger and D. S. McLachlan, Solid State Commun. 13, 1563 (1973).
[52]G. J. Nieuwenhuys, Phys. Lett. A 43, 301 (1973).
[53]G. J. Nieuwenhuys and B. M. Boerstoel, Phys. Lett. A 33, 281 (1970).
[54]M. P. Kawatra, J. I. Budnick, and J. A. Mydosh, Phys. Rev. B 2, 1587 (1970). The relative width $\Delta T/T_C$ of $d\rho_m/dT$ is reported to decrease with increasing concentration.
[55]A plot of σ_s versus, e.g., $(T/T_C)^2$ shows that this temperature dependence is less appropriate than $(T/T_C)^{3/2}$. Furthermore, the resistivity also varies as $(T/T_C)^{3/2}$, in agreement with the same theory that predicts the temperature dependence of σ_s (Ref. 57).
[56]G. Williams and J. W. Loram, J. Phys. F 1, 434 (1971).
[57]H. S. D. Cole and R. E. Turner, J. Phys. C 2, 124 (1969); see also, P. D. Long and R. E. Turner, J. Phys. F Suppl. 2, S137 (1970).
[58]Williams *et al.* (Ref. 15) experimentally determined the AF interaction energy from the magnetoresistance of a Pd(Mn) alloy. They obtained $E_{\text{int}} \approx 14$ K, i.e., a factor of 4 smaller than our value, probably owing to the lower maximum field available. Furthermore, their assumption that $\Delta\rho(H)$ varies as $\exp(-g\mu_B SH/E_{\text{int}})$ in the MFM approximation is incorrect.
[59]B. Caroli, J. Phys. Chem. Solids 28, 1427 (1967).
[60]H. Cottet, Ph.D. thesis (University of Geneva, 1971) (unpublished).
[61]H. Hasegawa, Prog. Theor. Phys. 21, 483 (1959).
[62]B. R. Coles, H. Jamieson, R. H. Taylor, and A. Tari (unpublished).
[63]R. H. Taylor and B. R. Coles, J. Phys. F 4, 303 (1974).
[64]R. A. Devine (private communication to G. J. Nieuwenhuys).
[65]G. J. Nieuwenhuys (private communication).
[66]R. W. Cochrane and J. O. Ström-Olsen, in Ref. 17, Vol. 2, p. 427. R. W. Cochrane, F. T. Hedgcock, and J. O. Ström-Olsen, Phys. Rev. B 8, 4262 (1973); R. W. Cochrane, M. Plischke, and J. O. Ström-Olsen, Phys. Rev. B 9, 3013 (1974).